Lecture II
Ab initio Potential Energy Surfaces (and Dipole Moments) in High Dimensionality

- Direct dynamics” for QM?
- Fitting strategies
- Coordinates
- The curse of dimensionality
- Permutational invariance
- Direct fitting on n-mode grids

Abandon the PES?

Calculate *V*(Q) “on the fly”, aka “Ab initio Molecular Dynamics”, aka “Direct Dynamics”

Molecular Dynamics Calculations

Solve the classical equations of motion for each atom

For example, for atom number 3 we have to solve

$$m_3 \frac{d^2 x_3}{dt^2} = F_{x_3} = -\frac{\partial V(x_1, y_1, z_1, \ldots x_3, y_3, z_3, \ldots)}{\partial x_3}$$

$$m_3 \frac{d^2 y_3}{dt^2} = F_{y_3} = -\frac{\partial V(x_1, y_1, z_1, \ldots x_3, y_3, z_3, \ldots)}{\partial y_3}$$

$$m_3 \frac{d^2 z_3}{dt^2} = F_{z_3} = -\frac{\partial V(x_1, y_1, z_1, \ldots x_3, y_3, z_3, \ldots)}{\partial z_3}$$

$x_1(t), y_1(t), z_1(t); x_2(t), y_2(t), z_2(t); x_3(t), y_3(t), z_3(t); \ldots$ **Classical Trajectory**

Need to run 10^3 - 10^4 trajectories for proper averaging over initial conditions

$$x_1(t=0), y_1(0), z_1(0); x_2(0), y_2(0), z_2(0); x_3(0), y_3(0), z_3(0); \ldots$$

$$\dot{x}_1(t=0), \dot{y}_1(0), \dot{z}_1(0); \dot{x}_2(0), \dot{y}_2(0), \dot{z}_2(0); \dot{x}_3(0), \dot{y}_3(0), \dot{z}_3(0); \ldots$$

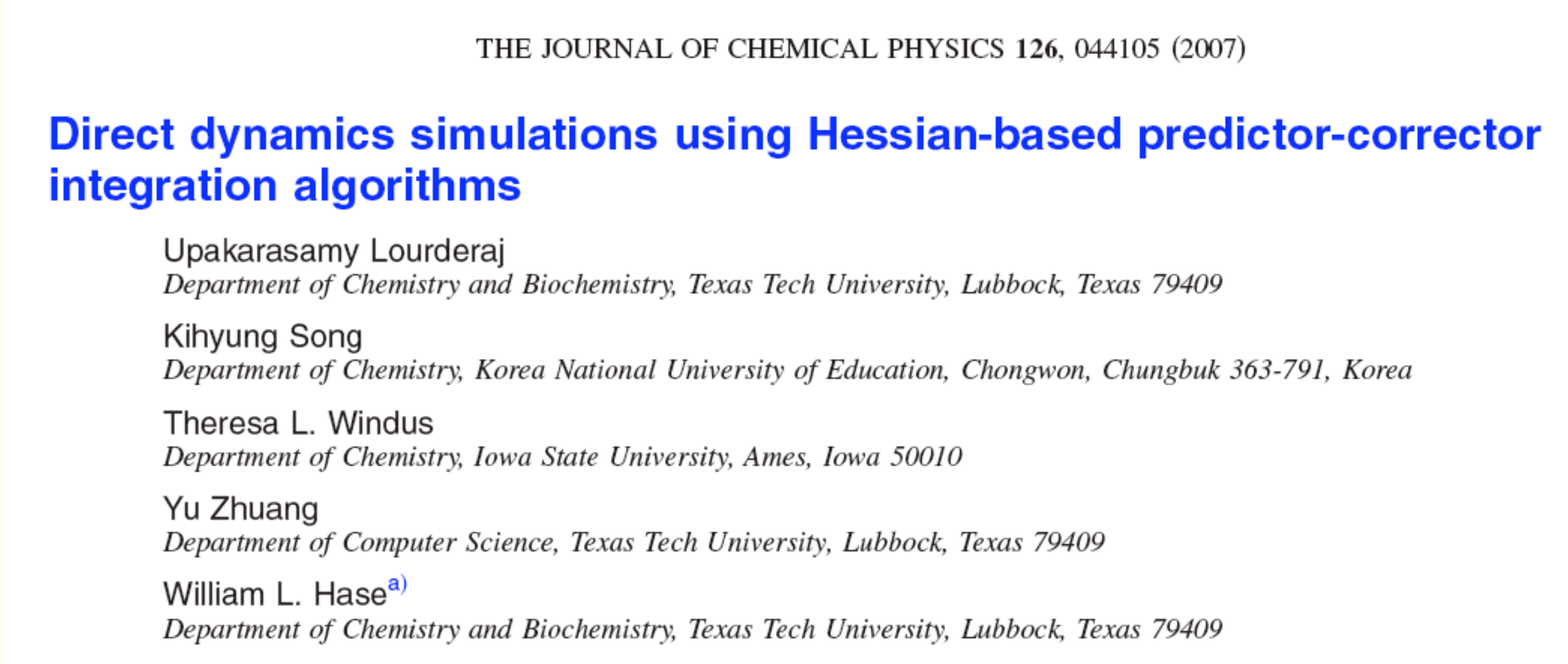

THE JOURNAL OF CHEMICAL PHYSICS **126**, 044105 (2007)

Direct dynamics simulations using Hessian-based predictor-corrector integration algorithms

Upakarasamy Lourderaj
Department of Chemistry and Biochemistry, Texas Tech University, Lubbock, Texas 79409

Kihyung Song
Department of Chemistry, Korea National University of Education, Chongwon, Chungbuk 363-791, Korea

Theresa L. Windus
Department of Chemistry, Iowa State University, Ames, Iowa 50010

Yu Zhuang
Department of Computer Science, Texas Tech University, Lubbock, Texas 79409

William L. Hase[a)]
Department of Chemistry and Biochemistry, Texas Tech University, Lubbock, Texas 79409

Ab initio Molecular Dynamics (AIMD)

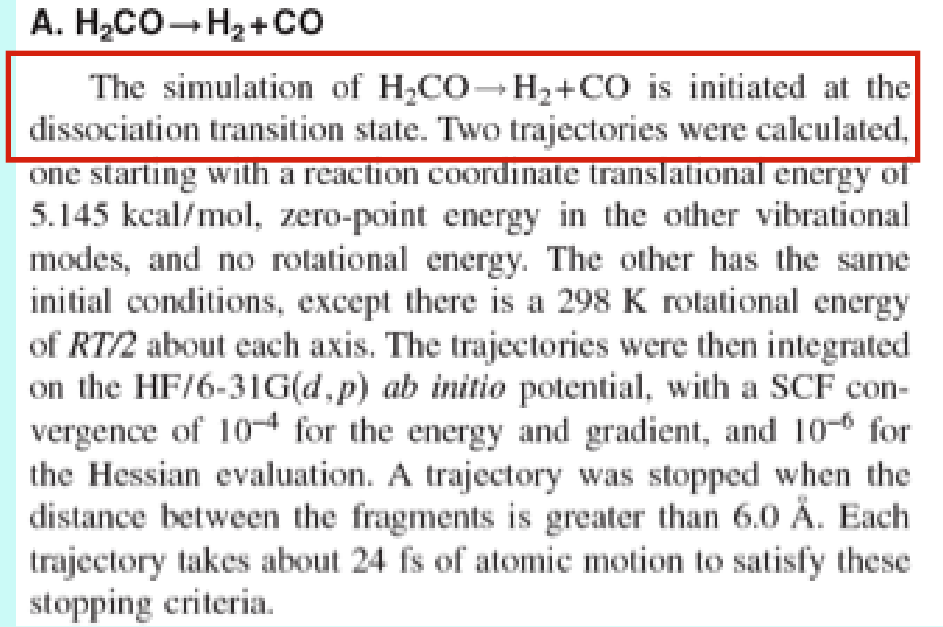

A. $H_2CO \rightarrow H_2 + CO$

The simulation of $H_2CO \rightarrow H_2 + CO$ is initiated at the dissociation transition state. Two trajectories were calculated, one starting with a reaction coordinate translational energy of 5.145 kcal/mol, zero-point energy in the other vibrational modes, and no rotational energy. The other has the same initial conditions, except there is a 298 K rotational energy of *RT/2* about each axis. The trajectories were then integrated on the HF/6-31G(*d*,*p*) *ab initio* potential, with a SCF convergence of 10^{-4} for the energy and gradient, and 10^{-6} for the Hessian evaluation. A trajectory was stopped when the distance between the fragments is greater than 6.0 Å. Each trajectory takes about 24 fs of atomic motion to satisfy these stopping criteria.

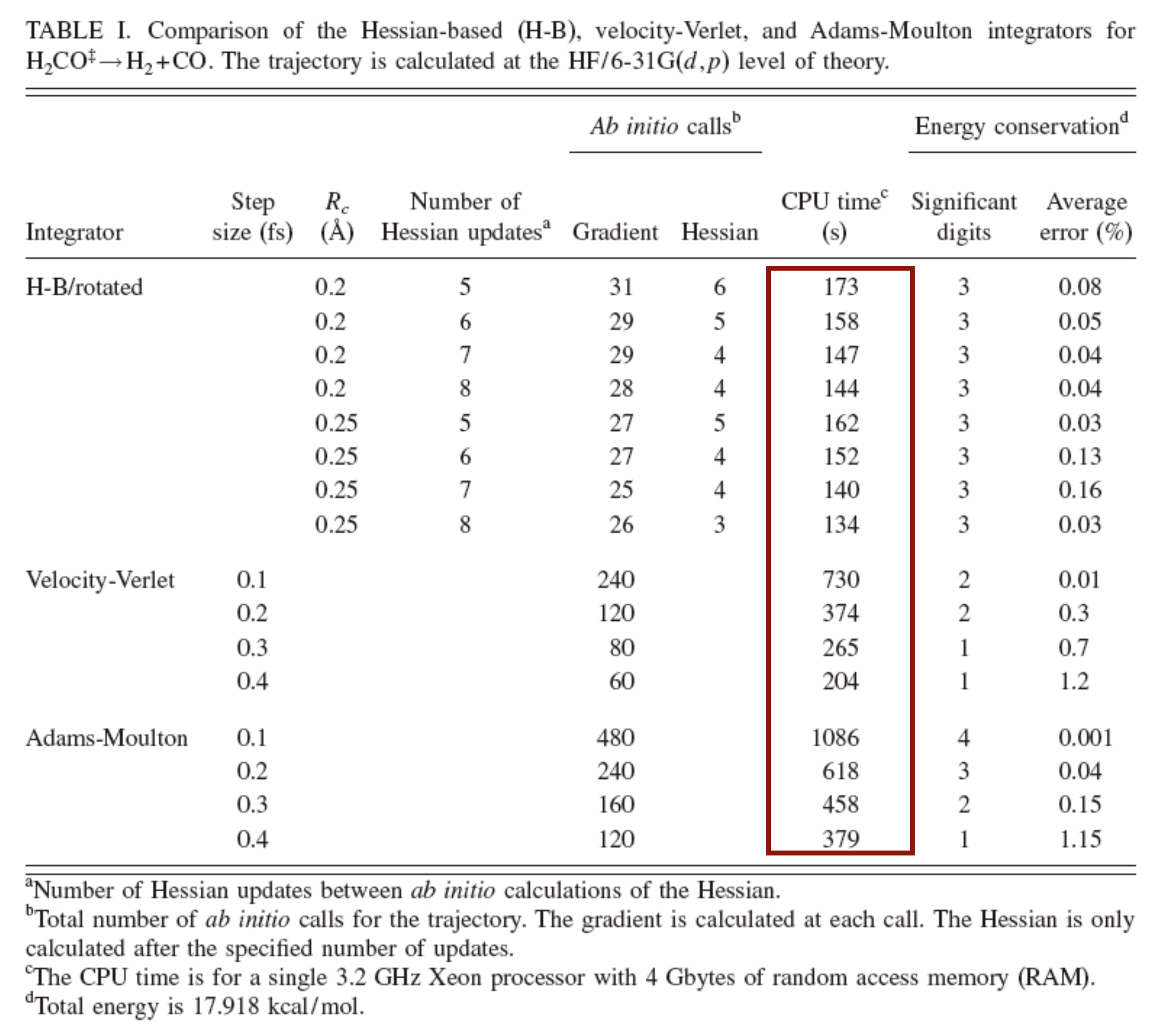

TABLE I. Comparison of the Hessian-based (H-B), velocity-Verlet, and Adams-Moulton integrators for $H_2CO^{\ddagger} \rightarrow H_2 + CO$. The trajectory is calculated at the HF/6-31G(*d*,*p*) level of theory.

				Ab initio calls[b]			Energy conservation[d]	
Integrator	Step size (fs)	R_c (Å)	Number of Hessian updates[a]	Gradient	Hessian	CPU time[c] (s)	Significant digits	Average error (%)
H-B/rotated		0.2	5	31	6	173	3	0.08
		0.2	6	29	5	158	3	0.05
		0.2	7	29	4	147	3	0.04
		0.2	8	28	4	144	3	0.04
		0.25	5	27	5	162	3	0.03
		0.25	6	27	4	152	3	0.13
		0.25	7	25	4	140	3	0.16
		0.25	8	26	3	134	3	0.03
Velocity-Verlet	0.1			240		730	2	0.01
	0.2			120		374	2	0.3
	0.3			80		265	1	0.7
	0.4			60		204	1	1.2
Adams-Moulton	0.1			480		1086	4	0.001
	0.2			240		618	3	0.04
	0.3			160		458	2	0.15
	0.4			120		379	1	1.15

[a] Number of Hessian updates between *ab initio* calculations of the Hessian.

[b] Total number of *ab initio* calls for the trajectory. The gradient is calculated at each call. The Hessian is only calculated after the specified number of updates.

[c] The CPU time is for a single 3.2 GHz Xeon processor with 4 Gbytes of random access memory (RAM).

[d] Total energy is 17.918 kcal/mol.

Ab initio Potential Energy Surfaces

Calculate sufficient number of (accurate) ε(Q) and then do an accurate fit of them. Easy for a diatomic, 10 pts enough

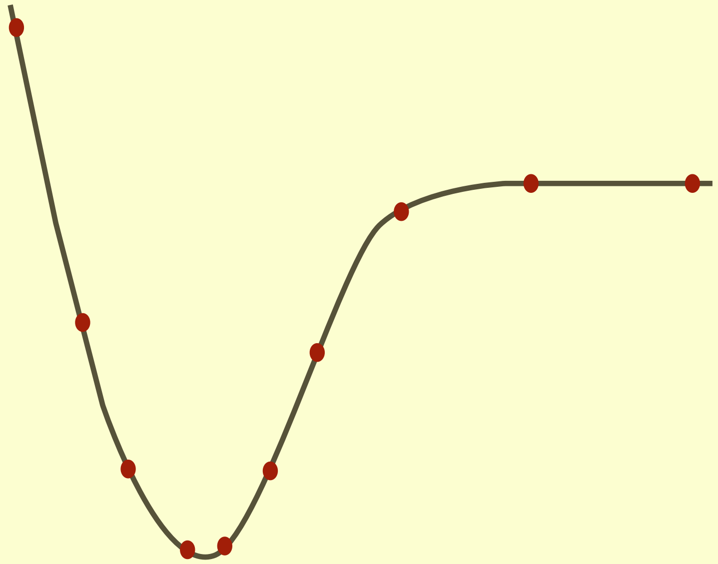

What about the generalization to polyatomics. Start with a triatomic, three degrees of freedom, 10^3 pts enough? Maybe more like 5,000.

Very feasible and can be used with a direct-product 3D spline

F. Lique, M. Jorfi, P. Honvault, P. Halvick, S. Y. Lin, H. Guo, D. Xie, J. Kłos, P. J. Dagdigian, and M. H. Alexander, J. Chem. Phys., 131, 221104 (2009), $O + OH \rightarrow O_2 + H$: A key reaction for interstellar and combustion chemistry. New theoretical results and comparison with experiment (18K points)

Ab initio Potential Energy Surfaces

Scaling looks very bad if we need 10 points per degree of freedom, e.g., tetraatomics need 10^6 electronic energies; $10^{(3N-6)}$ in general.

Models for PESs e.g., LEPS that contain a small number of parameters, generally non-linear, that were optimized either to experiment or to a small no. of ab initio data, e.g. barriers, etc.

Recent: Use low-level “AIMD” with parameter optimization based on high-level input, e.g., barrier height, exoergicity, etc. Specific Reaction Parameter method

Shepard interpolation of many quartic force fields
Interpolated moving least-squares

A Primer About Fitting

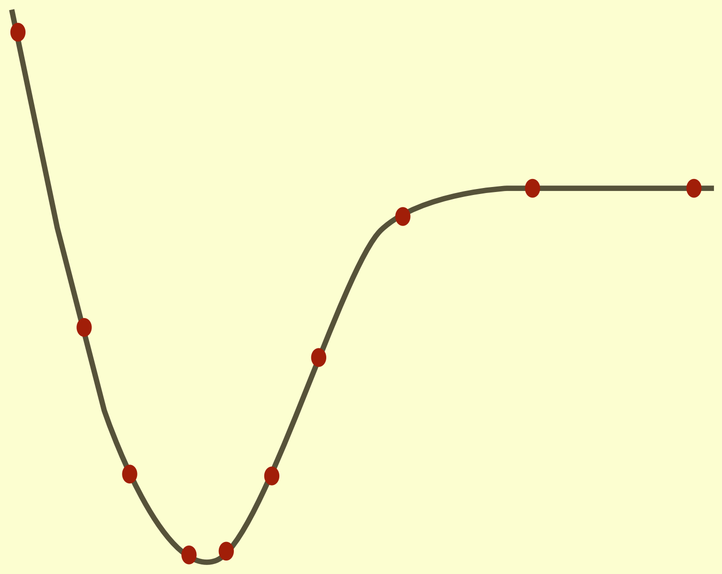

1d-spline

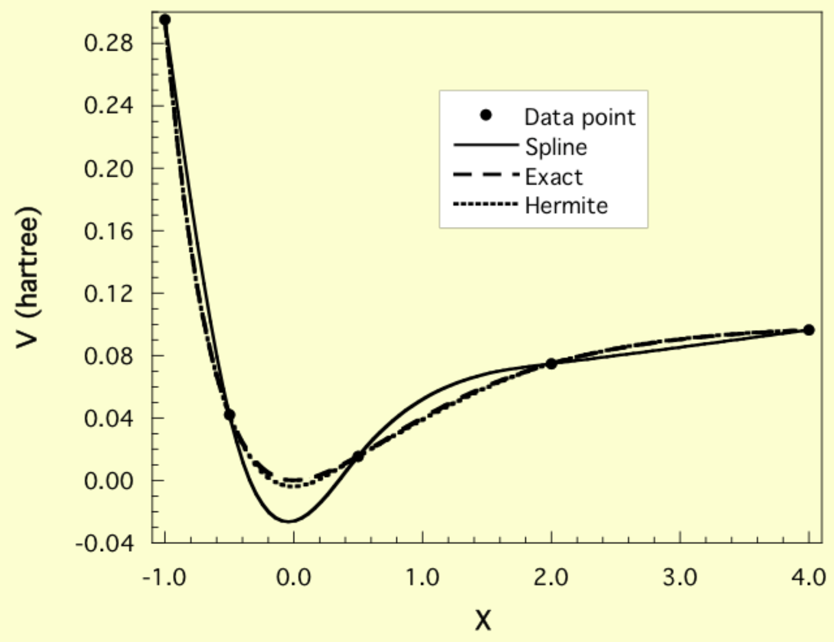

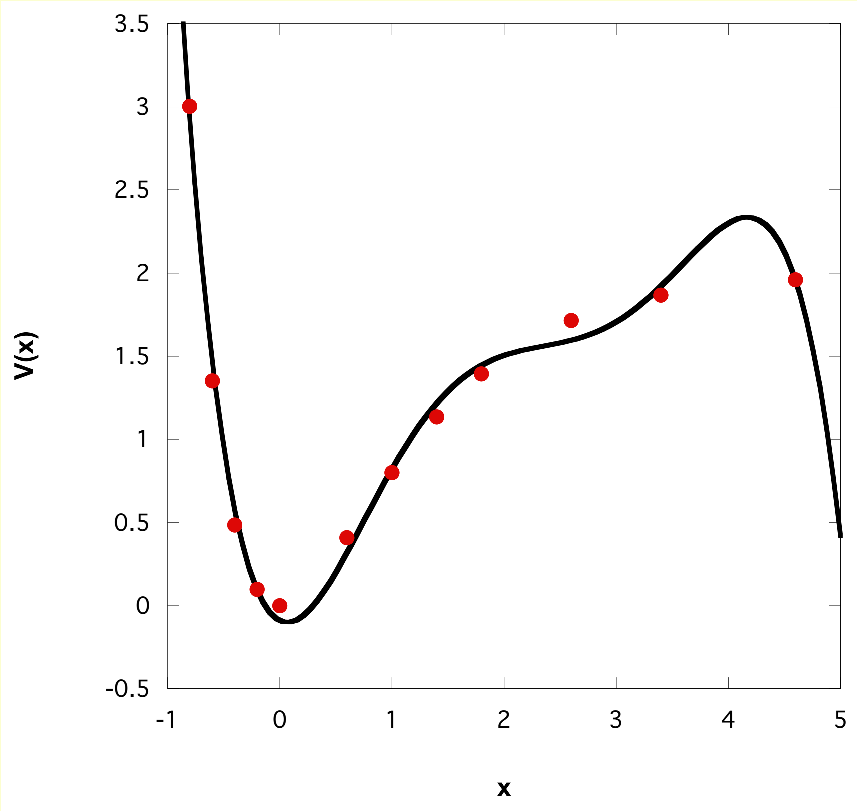

$$V(x) = 2[1 - e^{-x}]^2$$

Linear least squares 5th order poly in x

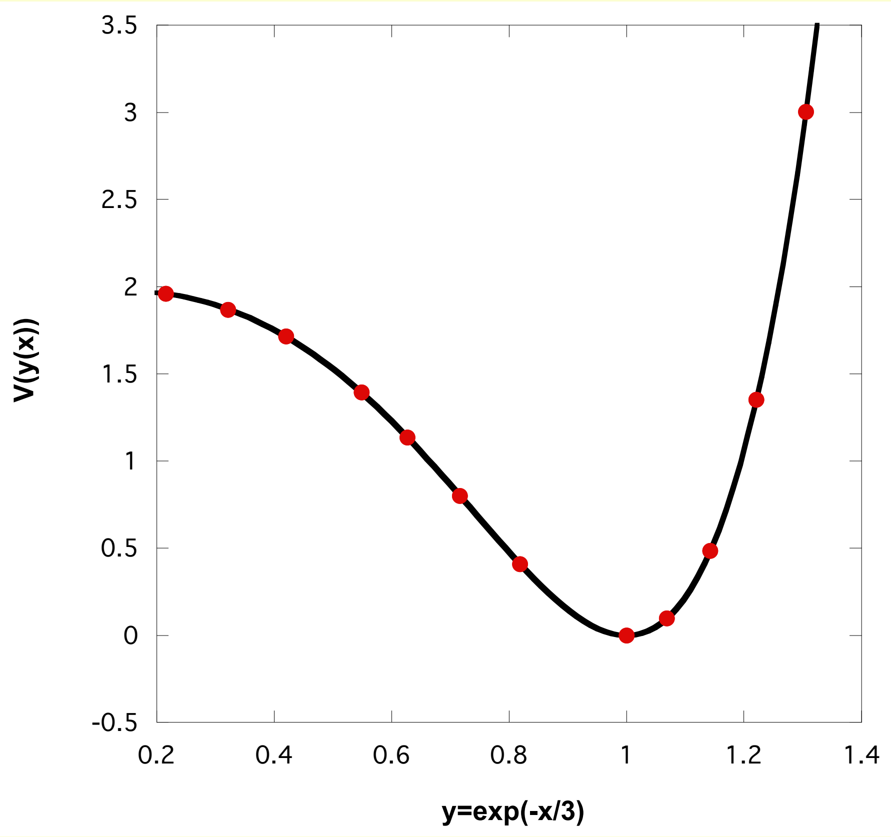

Linear least squares 5th order poly in “Morse” variable y=exp(-x/3).

Progress Using Permutational Invariance

As molecular systems get larger "atom degeneracy" increases, e.g., $H^+(H_2O)_2$, $H+CH_4$,CH_5^+.

The PES should be invariant wrt to all permutations of like atoms so ideally the fit should be as well. Exploit this in the fitting basis.

- Far fewer configurations than the 10^{3N-6} are needed
- Data can be scattered (maybe from low-level AIMD)
- Fits are more accurate (nature "knows" about symmetry)
- Fits accurately predict stationary points

Require V to be invariant under all permutations of like atoms

CH_5^+ – S_5

$H_5O_2^+$ – $S_5 \times S_2$

$H_3O_2^-$ – $S_3 \times S_2$

Need a set of variables that is closed under permutations

All internuclear distances are such a set.

Collaboration with Bas Braams (applied mathematician) & problem is "solved" but requires a symbolic algebra code, e.g, Magma.

Some simple examples: H_2CO and C_2H_2

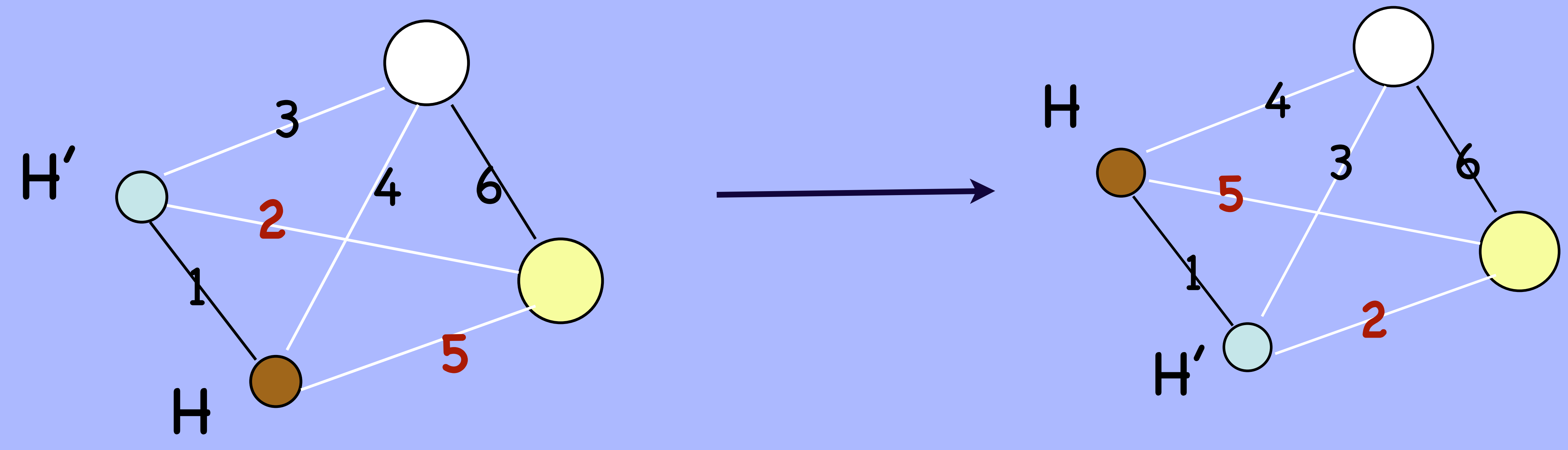

$$V(r_1\cdots r_6)=\sum_{n_1,n_2\dots n_6} C_{n_1\dots n_6}\, S\{y_1^{n_1}y_2^{n_2}y_3^{n_3}y_4^{n_4}y_5^{n_5}y_6^{n_6}\}$$

$$y=1-e^{-a(r-r_0)};\quad y=\frac{r-r_e}{r};etc$$

$$C_{n_1\dots n_6}\, y_1^{n_1} y_6^{n_6}(y_2^{n_2}y_3^{n_3}y_4^{n_4}y_5^{n_5}+y_2^{n_5}y_3^{n_4}y_4^{n_3}y_5^{n_2})$$

H(1) H(2) C(3) O(4)

$r_{12}\, r_{13}\, r_{14}\, r_{23}\, r_{24}\, r_{34}$:

$$\boxed{r_{12}^{n_1} r_{13}^{n_2} r_{14}^{n_3} r_{23}^{n_4} r_{24}^{n_5} r_{34}^{n_6}}$$

$$V(r_{12}, r_{13}, r_{14}, r_{23}, r_{24}, r_{34}) = \sum_{\boldsymbol{n}} C_{\boldsymbol{n}} (y_{12}^{n_1} y_{34}^{n_6} y_{13}^{n_2} y_{14}^{n_3} y_{23}^{n_4} y_{24}^{n_5})$$

H(2) H(1) C(3) O(4)

$r_{12}\, r_{23}\, r_{24}\, r_{13}\, r_{14}\, r_{34}$:

$$r_{12}^{n_1} r_{23}^{n_2} r_{24}^{n_3} r_{13}^{n_4} r_{14}^{n_5} r_{34}^{n_6} \quad \rightarrow \quad \boxed{r_{12}^{n_1} r_{13}^{n_4} r_{14}^{n_5} r_{23}^{n_2} r_{24}^{n_3} r_{34}^{n_6}}$$

$$\rightarrow \quad r_{12}^{n_1} r_{13}^{n_2} r_{14}^{n_3} r_{23}^{n_4} r_{24}^{n_5} r_{34}^{n_6} + r_{12}^{n_1} r_{13}^{n_4} r_{14}^{n_5} r_{23}^{n_2} r_{24}^{n_3} r_{34}^{n_6} =$$

$$r_{12}^{n_1} r_{34}^{n_6} (r_{13}^{n_2} r_{14}^{n_3} r_{23}^{n_4} r_{24}^{n_5} + r_{13}^{n_4} r_{14}^{n_5} r_{23}^{n_2} r_{24}^{n_3})$$

$$V(r_{12}, r_{13}, r_{14}, r_{23}, r_{24}, r_{34}) = \sum_{\boldsymbol{n}} C_{\boldsymbol{n}} [y_{12}^{n_1} y_{34}^{n_6} (y_{13}^{n_2} y_{14}^{n_3} y_{23}^{n_4} y_{24}^{n_5} + y_{13}^{n_4} y_{14}^{n_5} y_{23}^{n_2} y_{24}^{n_3})]$$

Monomial Symmetrization C(1)C(2)H(3)H(4)

$$V = \sum_{m=a+b+c+d+e+f} C_{abcdef} [y_{12}^{a} y_{13}^{b} y_{14}^{c} y_{23}^{d} y_{24}^{e} y_{34}^{f}]$$

$$y_{ij} = exp(-r_{ij}/a)$$

$$V = \sum_{m=0}^{N} D_{abcdef} S[y_{12}^{a} y_{13}^{b} y_{14}^{c} y_{23}^{d} y_{24}^{e} y_{34}^{f}]$$

S is an operator that generates a sum of monomials that is invariant wrt to the 2!2! = 4 permutations

Monomial Symmetrization

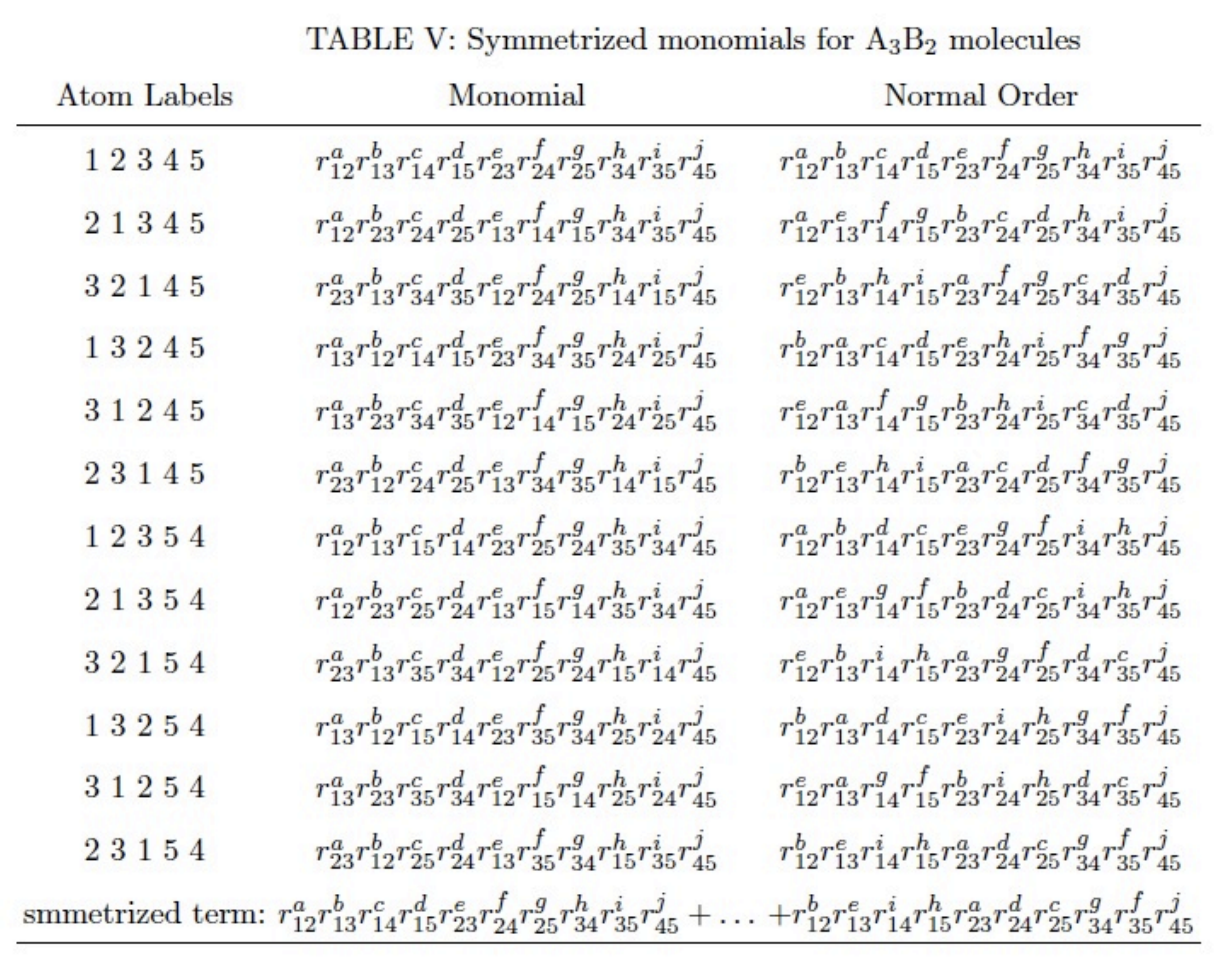

TABLE V: Symmetrized monomials for A_3B_2 molecules

Atom Labels	Monomial	Normal Order
1 2 3 4 5	$r_{12}^a r_{13}^b r_{14}^c r_{15}^d r_{23}^e r_{24}^f r_{25}^g r_{34}^h r_{35}^i r_{45}^j$	$r_{12}^a r_{13}^b r_{14}^c r_{15}^d r_{23}^e r_{24}^f r_{25}^g r_{34}^h r_{35}^i r_{45}^j$
2 1 3 4 5	$r_{12}^a r_{23}^b r_{24}^c r_{25}^d r_{13}^e r_{14}^f r_{15}^g r_{34}^h r_{35}^i r_{45}^j$	$r_{12}^a r_{13}^e r_{14}^f r_{15}^g r_{23}^b r_{24}^c r_{25}^d r_{34}^h r_{35}^i r_{45}^j$
3 2 1 4 5	$r_{23}^a r_{13}^b r_{34}^c r_{35}^d r_{12}^e r_{24}^f r_{25}^g r_{14}^h r_{15}^i r_{45}^j$	$r_{12}^e r_{13}^b r_{14}^h r_{15}^i r_{23}^a r_{24}^f r_{25}^g r_{34}^c r_{35}^d r_{45}^j$
1 3 2 4 5	$r_{13}^a r_{12}^b r_{14}^c r_{15}^d r_{23}^e r_{34}^f r_{35}^g r_{24}^h r_{25}^i r_{45}^j$	$r_{12}^b r_{13}^a r_{14}^c r_{15}^d r_{23}^e r_{24}^h r_{25}^i r_{34}^f r_{35}^g r_{45}^j$
3 1 2 4 5	$r_{13}^a r_{23}^b r_{34}^c r_{35}^d r_{12}^e r_{14}^f r_{15}^g r_{24}^h r_{25}^i r_{45}^j$	$r_{12}^e r_{13}^a r_{14}^f r_{15}^g r_{23}^b r_{24}^h r_{25}^i r_{34}^c r_{35}^d r_{45}^j$
2 3 1 4 5	$r_{23}^a r_{12}^b r_{24}^c r_{25}^d r_{13}^e r_{34}^f r_{35}^g r_{14}^h r_{15}^i r_{45}^j$	$r_{12}^b r_{13}^e r_{14}^h r_{15}^i r_{23}^a r_{24}^c r_{25}^d r_{34}^f r_{35}^g r_{45}^j$
1 2 3 5 4	$r_{12}^a r_{13}^b r_{15}^c r_{14}^d r_{23}^e r_{25}^f r_{24}^g r_{35}^h r_{34}^i r_{45}^j$	$r_{12}^a r_{13}^b r_{14}^d r_{15}^c r_{23}^e r_{24}^g r_{25}^f r_{34}^i r_{35}^h r_{45}^j$
2 1 3 5 4	$r_{12}^a r_{23}^b r_{25}^c r_{24}^d r_{13}^e r_{15}^f r_{14}^g r_{35}^h r_{34}^i r_{45}^j$	$r_{12}^a r_{13}^e r_{14}^g r_{15}^f r_{23}^b r_{24}^d r_{25}^c r_{34}^i r_{35}^h r_{45}^j$
3 2 1 5 4	$r_{23}^a r_{13}^b r_{35}^c r_{34}^d r_{12}^e r_{25}^f r_{24}^g r_{15}^h r_{14}^i r_{45}^j$	$r_{12}^e r_{13}^b r_{14}^i r_{15}^h r_{23}^a r_{24}^g r_{25}^f r_{34}^d r_{35}^c r_{45}^j$
1 3 2 5 4	$r_{13}^a r_{12}^b r_{15}^c r_{14}^d r_{23}^e r_{35}^f r_{34}^g r_{25}^h r_{24}^i r_{45}^j$	$r_{12}^b r_{13}^a r_{14}^d r_{15}^c r_{23}^e r_{24}^i r_{25}^h r_{34}^g r_{35}^f r_{45}^j$
3 1 2 5 4	$r_{13}^a r_{23}^b r_{35}^c r_{34}^d r_{12}^e r_{15}^f r_{14}^g r_{25}^h r_{24}^i r_{45}^j$	$r_{12}^e r_{13}^a r_{14}^g r_{15}^f r_{23}^b r_{24}^i r_{25}^h r_{34}^d r_{35}^c r_{45}^j$
2 3 1 5 4	$r_{23}^a r_{12}^b r_{25}^c r_{24}^d r_{13}^e r_{35}^f r_{34}^g r_{15}^h r_{35}^i r_{45}^j$	$r_{12}^b r_{13}^e r_{14}^i r_{15}^h r_{23}^a r_{24}^d r_{25}^c r_{34}^g r_{35}^f r_{45}^j$
smmetrized term: $r_{12}^a r_{13}^b r_{14}^c r_{15}^d r_{23}^e r_{24}^f r_{25}^g r_{34}^h r_{35}^i r_{45}^j + \ldots + r_{12}^b r_{13}^e r_{14}^i r_{15}^h r_{23}^a r_{24}^d r_{25}^c r_{34}^g r_{35}^f r_{45}^j$		

FCH_4 Twenty Four Permutations of 15 r_{ij}

Atom Labels H(0) H(1) H(2) H(3) C(4) F(5)

$$r_{01}r_{02}r_{03}r_{04}r_{05}r_{12}r_{13}r_{14}r_{15}r_{23}r_{24}r_{25}r_{34}r_{35}r_{45}$$

Atom Labels H(1) H(0) H(2) H(3) C(4) F(5)

$$r_{01}r_{12}r_{13}r_{14}r_{15}r_{02}r_{03}r_{04}r_{05}r_{23}r_{24}r_{25}r_{34}r_{35}r_{45}$$

etc. A more elegant and efficient way to achieve this permutational invariance is from invariant polynomial theory in terms of (15) primary invariants (p) and secondary invariants q.

$$V(\mathbf{y}) = \sum_{\alpha=1}^{M} \mathrm{poly}_{\alpha}(\mathbf{p}(\mathbf{y}))q_{\alpha}(\mathbf{y}),$$

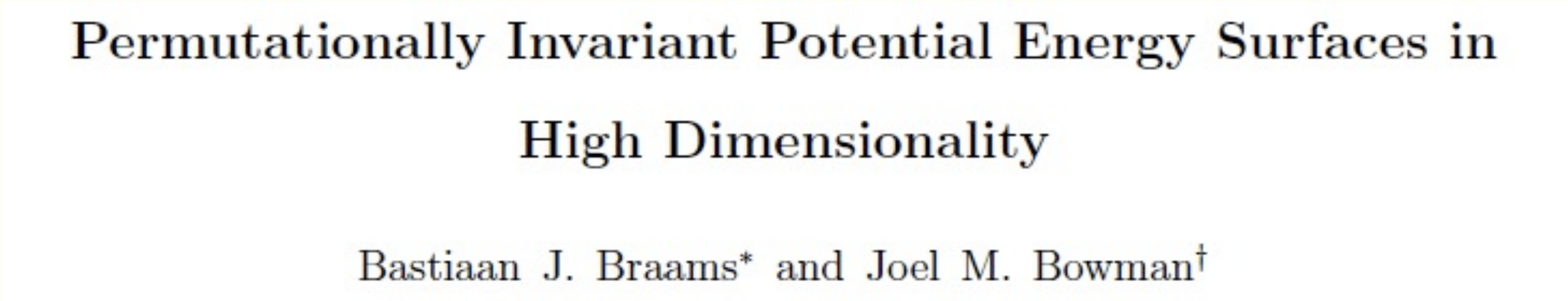

Permutationally Invariant Potential Energy Surfaces in High Dimensionality

Bastiaan J. Braams* and Joel M. Bowman†

Int. Rev. Phys. Chem. **28**, 577–606 (2009).

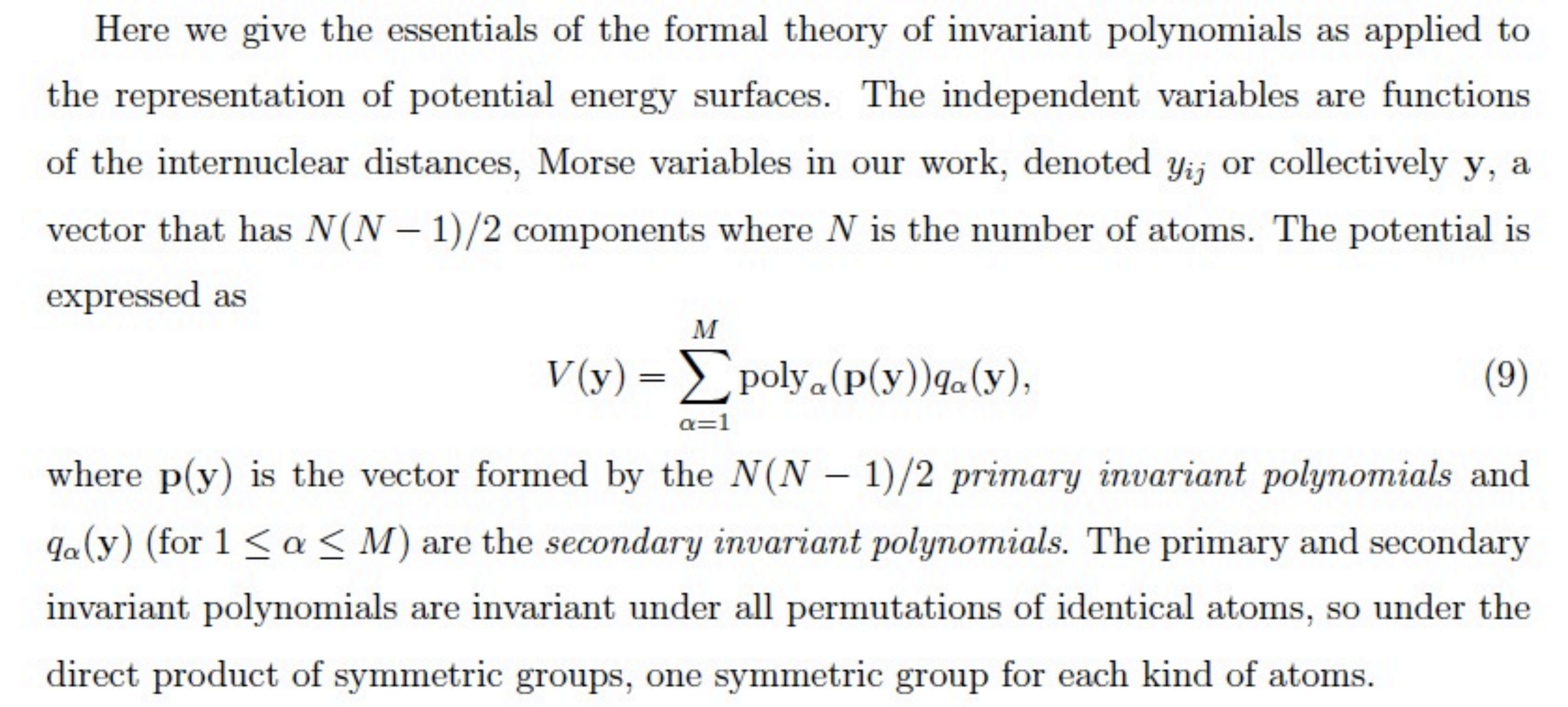

Here we give the essentials of the formal theory of invariant polynomials as applied to the representation of potential energy surfaces. The independent variables are functions of the internuclear distances, Morse variables in our work, denoted y_{ij} or collectively $\mathbf{y}$, a vector that has $N(N-1)/2$ components where N is the number of atoms. The potential is expressed as

$$V(\mathbf{y}) = \sum_{\alpha=1}^{M} \mathrm{poly}_{\alpha}(\mathbf{p}(\mathbf{y}))q_{\alpha}(\mathbf{y}), \tag{9}$$

where $\mathbf{p}(\mathbf{y})$ is the vector formed by the $N(N-1)/2$ *primary invariant polynomials* and $q_{\alpha}(\mathbf{y})$ (for $1 \leq \alpha \leq M$) are the *secondary invariant polynomials*. The primary and secondary invariant polynomials are invariant under all permutations of identical atoms, so under the direct product of symmetric groups, one symmetric group for each kind of atoms.

Permuationally invariant polynomials

- Cartesian coords $\mathbf{X} \Rightarrow \{r_{ij} = |\mathbf{x_i} - \mathbf{x_j}|\} \Leftrightarrow \{y_{ij} = \exp\left(-\frac{r_{ij}}{\lambda}\right)\}$
- The all-atom potential is represented as,

$$V(\mathbf{y}) = \sum_J c_J \cdot b_J(\mathbf{y})$$

where

$$b_J(\mathbf{y}) = p_1^{n_1}(\mathbf{y}) \cdot p_2^{n_2}(\mathbf{y}) \cdots p_k^{n_k}(\mathbf{y}) \cdot q_\beta(\mathbf{y})$$

$$J = (n_1, n_2, \cdots, n_k, \beta);\ n_i = 0, 1, \cdots$$

$$d = \sum_{i=1}^{k} n_i \deg(p_i) + \deg(q_\beta); \quad d \leq D_{\max}$$

There are $\frac{N(N-1)}{2}$ $\underline{\text{primary invariants } p_i(\mathbf{y})}$, e.g. $p_1 = y_{12} + y_{13} + y_{23}$ and a certain number of $\underline{\text{secondary invariants } q_\beta(\mathbf{y})}$.

Details of Current Library

- Bases for up to ten atoms (but not all possible symmetric groups, esp for larger molecules.)

- Bases also available for Dipole Moment Surfaces

- Large library which until recently had to be compiled in total for each PES.

- New python script written by Yimin Wang to extract relevant routines for a given PES.

Some Practical Points

1. Generate data, often from AIMD
2. Add fragment channel data
3. Perform a fit
4. Locate stationary points

5. Add data around stationary points of interest
6. Run MD or DMC or ... to find problematic regions
7. Add data there
8. Re-fit

Replace low-level ab initio/DFT data with high level ab initio energies (maybe gradients too) and do final fit, analyze, etc.

No. of configurations ranges from ca 10 000 to 100 000

An *ab initio*-Based Global Potential Energy Surface Describing $CH_5^+ \rightarrow CH_3^+ + H_2$

[40 000 CCSD(T)/aug-cc-pVTZ energies]

Zhong Jin, Bastiaan J. Braams and Joel M. Bowman[a]

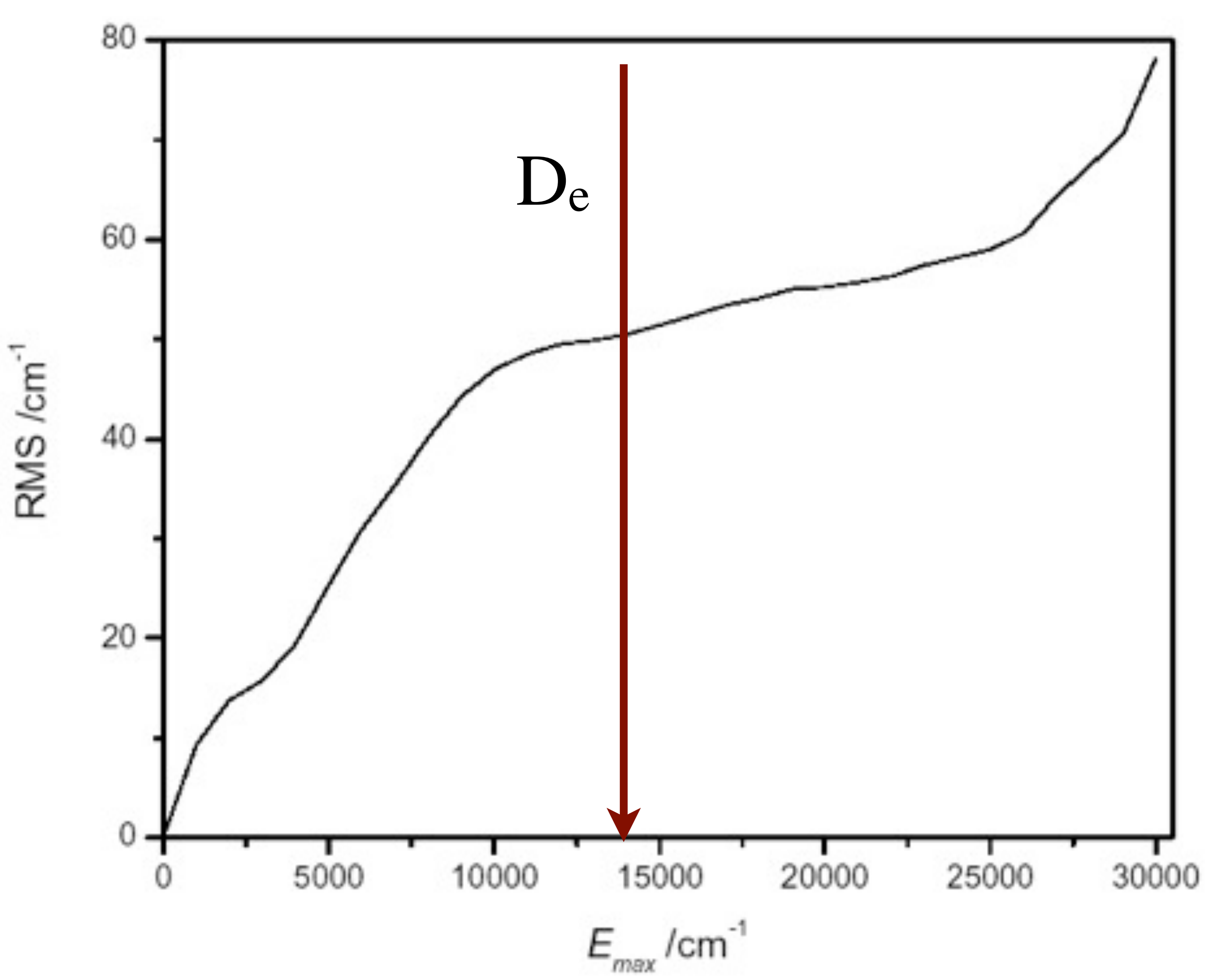

C_s(SP)/cm^{-1}	C_{2v}(SP)/cm^{-1}
34*	286*
29 (PES)	341

(12 dofs, 15 r_{ij})

---

* Müller, H.; Kutzelnigg, W.; Noga, J.; Klopper, W. *J. Chem. Phys.* **1997**,

$H_5O_2^+$ (15 dofs)

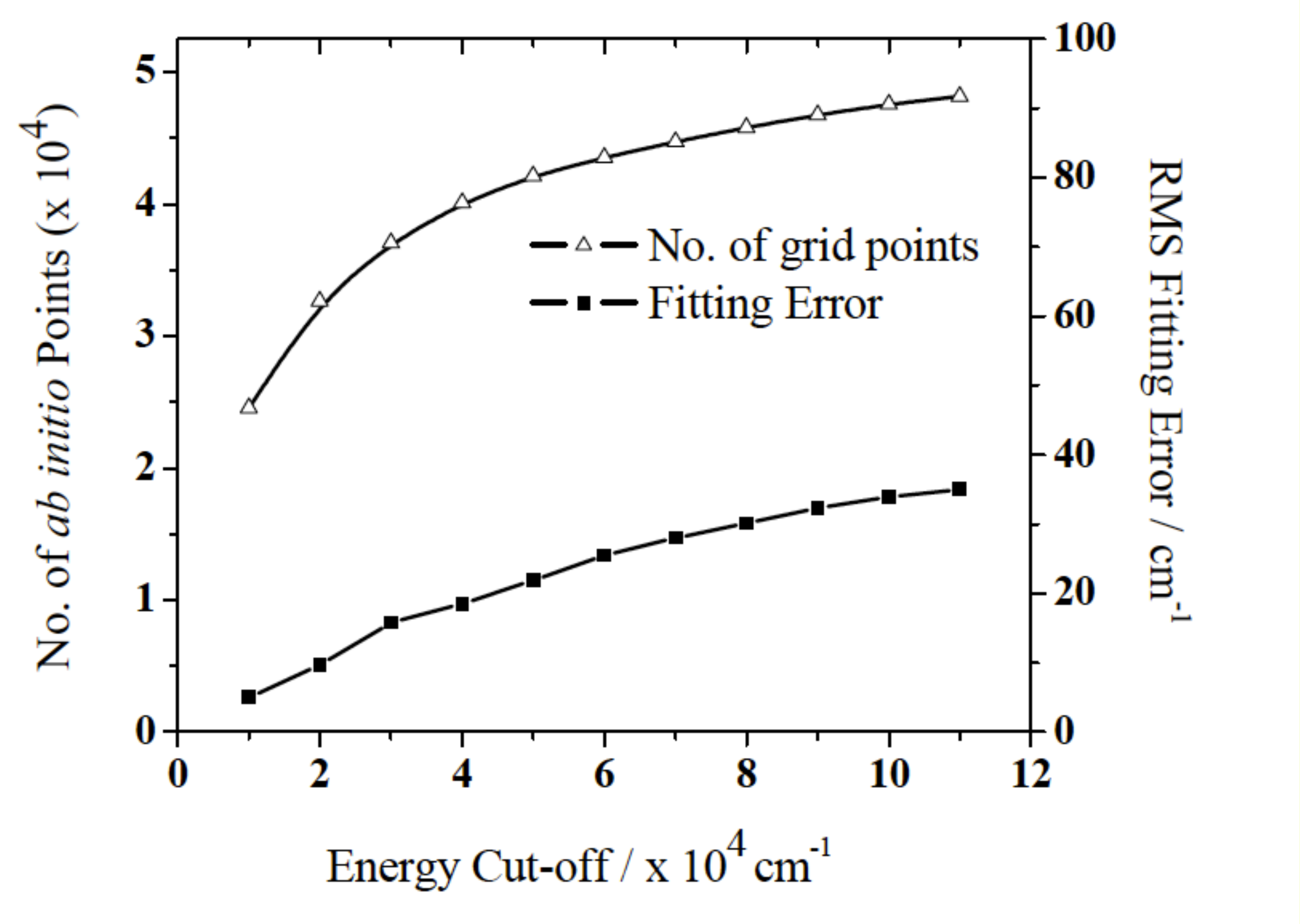

Huang, Braams, Bowman (2004) also DMS

$H_5O_2^+$

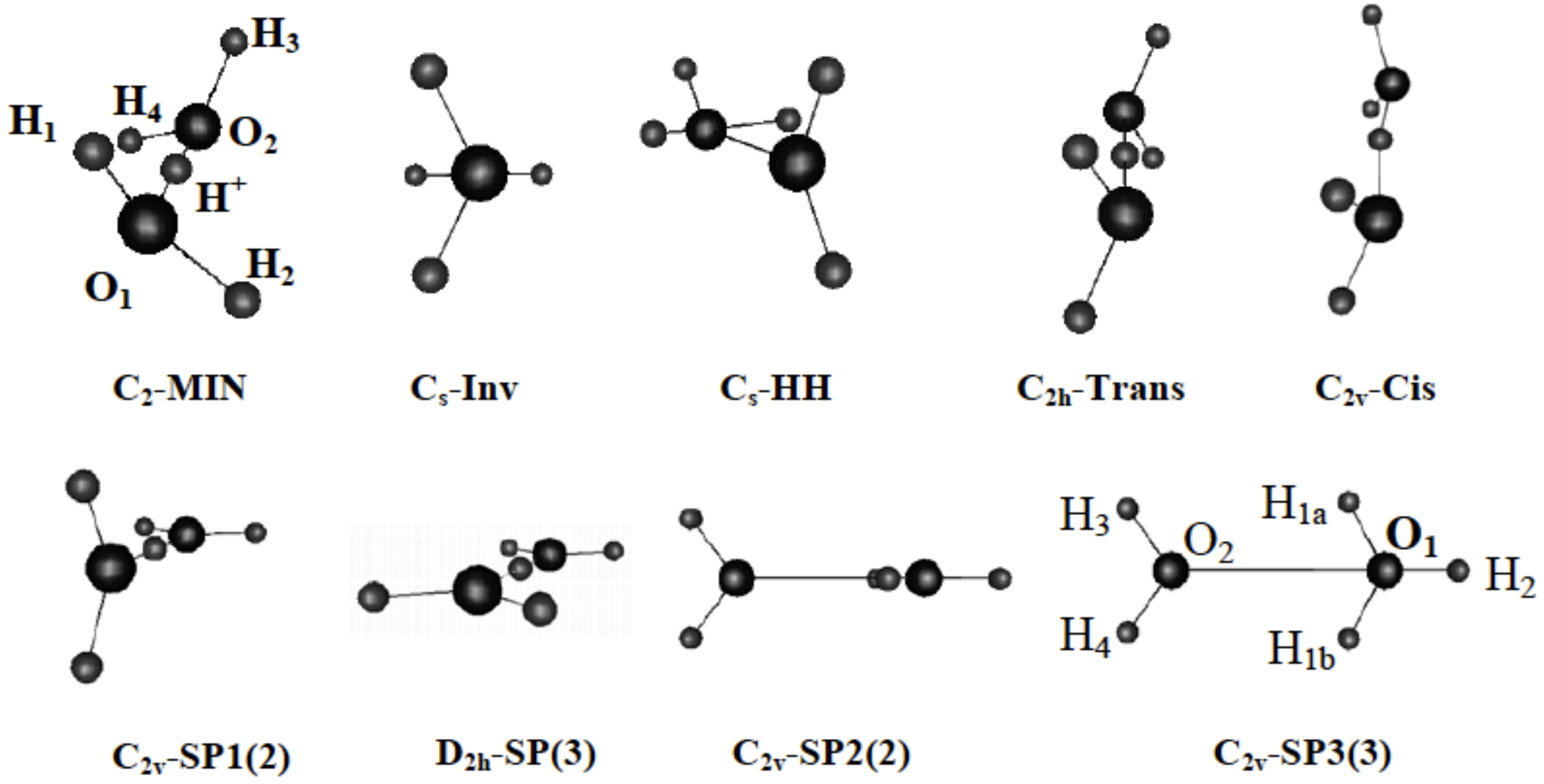

C_2-MIN

C_s-Inv

C_s-HH

C_{2h}-Trans

C_{2v}-Cis

C_{2v}-SP1(2)

D_{2h}-SP(3)

C_{2v}-SP2(2)

C_{2v}-SP3(3)

PESs To Date

Unimolecular

CH_5^+

H_5^+ H_7^+

$CHOCH_2CHO$ (malonaldehyde) H-atom transfer.

$C_2H_3 \rightarrow H+C_2H_2$ and isomerization

$C_3H_5 \rightarrow H+C_3H_4$(isomers), $CH_3+C_2H_2$ & vinylidene

$CH_2CH_2OH \rightarrow OH+CH_2CH_2$, $H_2O+C_2H_3$, etc.

CH_5^+ (+ Cs) $\rightarrow [CH_5]^*$ H_2+CH_3, $H+CH_4$

H_3O^+ (+ Cs) $\rightarrow [H_3O]^*$ H_2+OH, H_2O+H

$CH_2O \rightarrow H_2+CO$, $H+HCO$ (Roaming)

$CH_3CHO \rightarrow$ many products (Roaming)

$CH_2CH_2OH \rightarrow$ products, $C_2H_3 + H_2O$

$CH_2OH/CH_3O \rightarrow H + CH_2O$

$H_5O_2^+ \rightarrow H_3O^+ + H_2O$

$H_2O(OH^-)$

H_2CO $S_1/T_1/S_0$

$(H_2O)_2$, $(H_2O)_3$

Na^+(H2O), Cl^-(H2O), F^-(H2O)

$HCl(H_2O)$

$CH_3OH \rightarrow CH_3+OH$

Bimolecular

$NO_2 + OH \rightarrow [HOONO, HONO_2] \rightarrow NO + HO_2$

Roaming mediated isomerization

$C+C_2H_2 \rightarrow$ *l*-C_3H, *c*-C_3H + H, C_3+H_2

$H_2O+D_2O \rightarrow 2HDO$

$OH^*+H_2 \rightarrow H_2O + H$, $OH + H_2$

$H+CD_4 \rightarrow HD + CD_3$

$F+CHD_3 \rightarrow HF + CD_3$, $DF + CHD_2$

$Cl + CH_4 \rightarrow HCl + CH_3$

$O(^3P) + CH_4 \rightarrow HCl + CH_3$

$O(^3P)+C_2H_4$ w/singlet $\rightarrow$ products

$O+NO_2 \rightarrow [NO_3] \rightarrow O_2+NO$

$OH+CO \rightarrow [HOCO] \rightarrow H+CO_2$

$H+HCN \rightarrow$[H2CN/HCNH] $\rightarrow H_2+CN$

HOCO Details

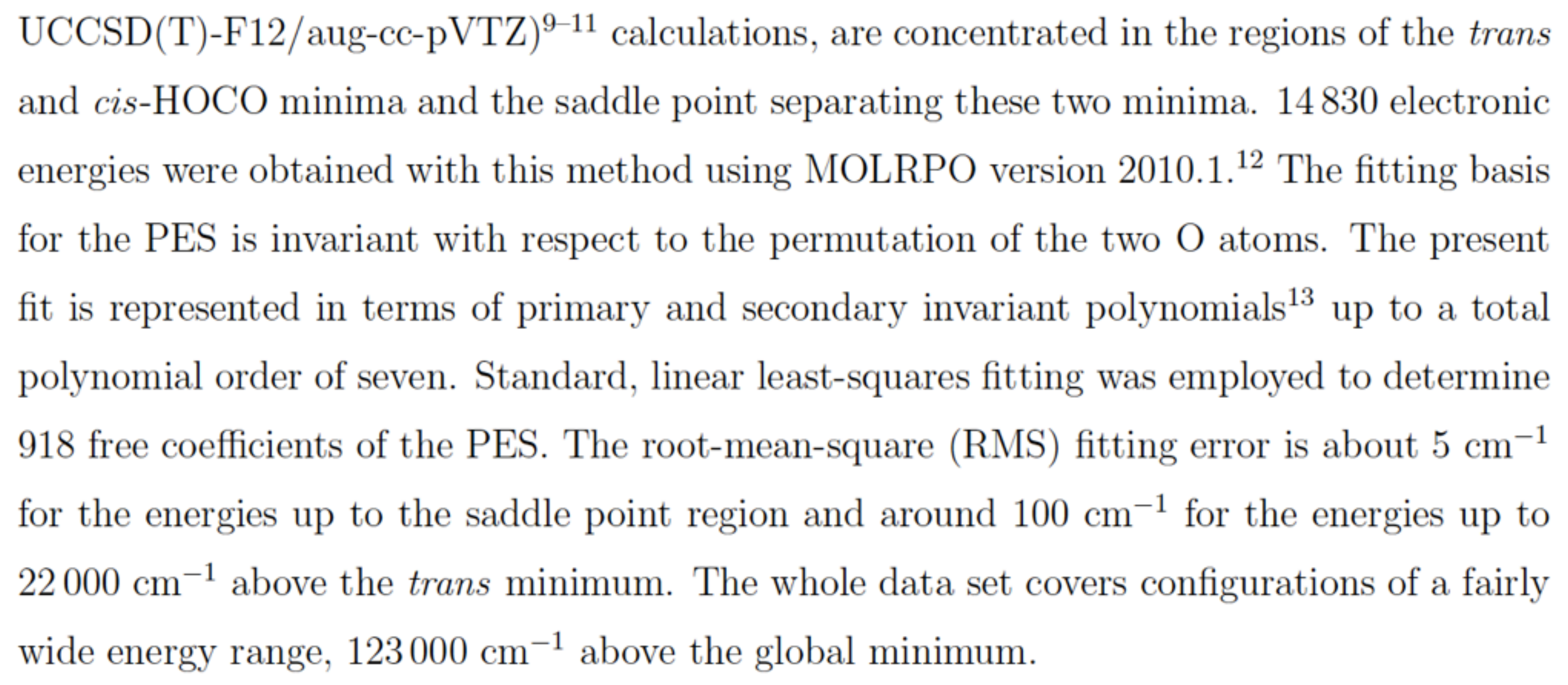

UCCSD(T)-F12/aug-cc-pVTZ)[9–11] calculations, are concentrated in the regions of the *trans* and *cis*-HOCO minima and the saddle point separating these two minima. 14 830 electronic energies were obtained with this method using MOLRPO version 2010.1.[12] The fitting basis for the PES is invariant with respect to the permutation of the two O atoms. The present fit is represented in terms of primary and secondary invariant polynomials[13] up to a total polynomial order of seven. Standard, linear least-squares fitting was employed to determine 918 free coefficients of the PES. The root-mean-square (RMS) fitting error is about 5 cm^{-1} for the energies up to the saddle point region and around 100 cm^{-1} for the energies up to 22 000 cm^{-1} above the *trans* minimum. The whole data set covers configurations of a fairly wide energy range, 123 000 cm^{-1} above the global minimum.

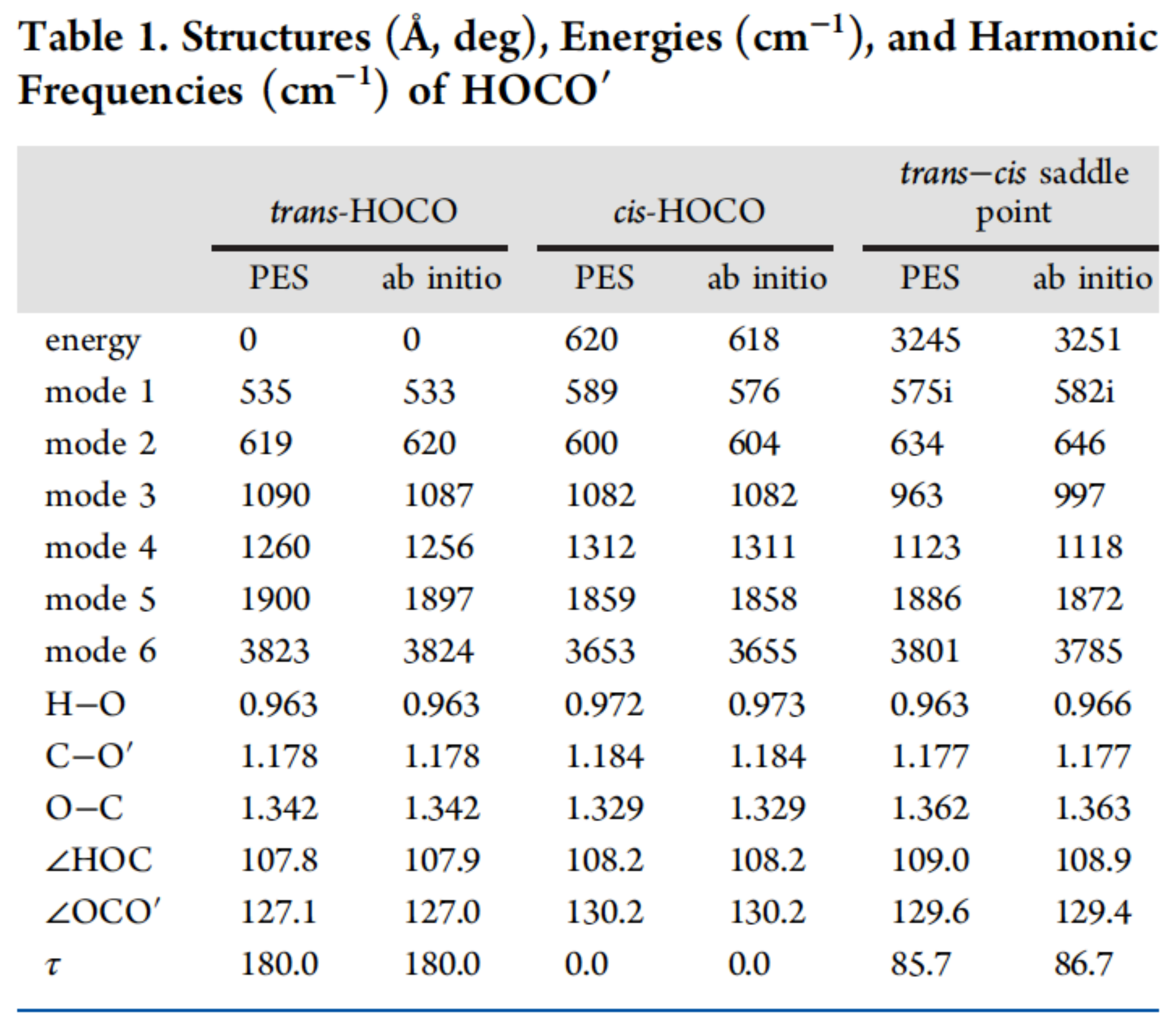

Table 1. Structures (Å, deg), Energies (cm^{-1}), and Harmonic Frequencies (cm^{-1}) of HOCO′

	trans-HOCO		*cis*-HOCO		*trans*–*cis* saddle point	
	PES	ab initio	PES	ab initio	PES	ab initio
energy	0	0	620	618	3245	3251
mode 1	535	533	589	576	575i	582i
mode 2	619	620	600	604	634	646
mode 3	1090	1087	1082	1082	963	997
mode 4	1260	1256	1312	1311	1123	1118
mode 5	1900	1897	1859	1858	1886	1872
mode 6	3823	3824	3653	3655	3801	3785
H–O	0.963	0.963	0.972	0.973	0.963	0.966
C–O′	1.178	1.178	1.184	1.184	1.177	1.177
O–C	1.342	1.342	1.329	1.329	1.362	1.363
∠HOC	107.8	107.9	108.2	108.2	109.0	108.9
∠OCO′	127.1	127.0	130.2	130.2	129.6	129.4
τ	180.0	180.0	0.0	0.0	85.7	86.7

Many-Body Expansion for N Monomers

$$V(1,\ldots,N) = \sum_{i=1} V^{(1)}(\mathbf{r}_i) + \sum_{i>j} V^{(2)}(\mathbf{r}_i,\mathbf{r}_j) + \sum_{i>j>k} V^{(3)}(\mathbf{r}_i,\mathbf{r}_j,\mathbf{r}_k) + \cdots$$

No. of r_{ij}s :	3	15	36
No. of terms :	N	N^2	N^3

$$V^{(1)}(\mathbf{r}_i) - \text{Electronic energy of monomer } i$$

$$V^{(2)}(\mathbf{r}_i,\mathbf{r}_j) - \text{Electronic energy of dimer } i,j \text{ - } [V^{(1)}(\mathbf{r}_i) + V^{(1)}(\mathbf{r}_j)]$$

$$V^{(3)}(\mathbf{r}_i,\mathbf{r}_j,\mathbf{r}_k) - \text{Electronic energy of trimer } i,j,k \text{ - } [V^{(1)}(\mathbf{r}_i) + V^{(1)}(\mathbf{r}_j) + V^{(1)}(\mathbf{r}_k)]$$

$$- [V^{(2)}(i,j) + V^{(2)}(i,k) + V^{(2)}(j,k)]$$

A single monomer is sufficient to get $V^{(1)}$(i)

A single dimer is sufficient to get $V^{(2)}$(i,j)

A single trimer is sufficient to get $V^{(3)}$(i,j,k)

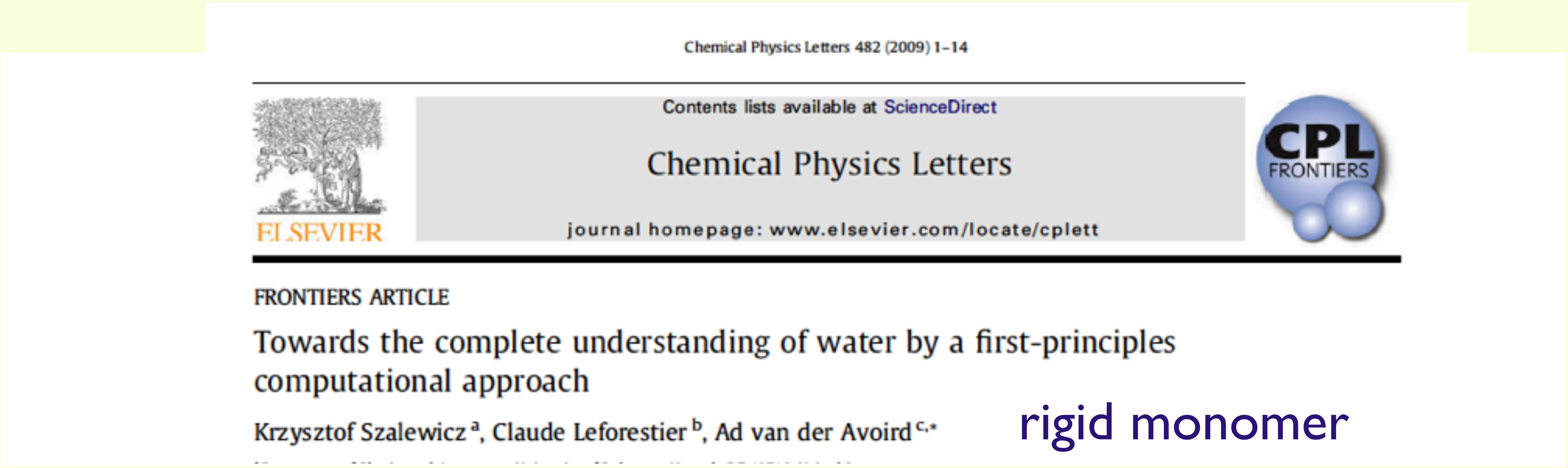

Chemical Physics Letters 482 (2009) 1–14

Contents lists available at ScienceDirect

Chemical Physics Letters

journal homepage: www.elsevier.com/locate/cplett

FRONTIERS ARTICLE

Towards the complete understanding of water by a first-principles computational approach

Krzysztof Szalewicz [a], Claude Leforestier [b], Ad van der Avoird [c,*]

rigid monomer

Earlier work by Xantheas

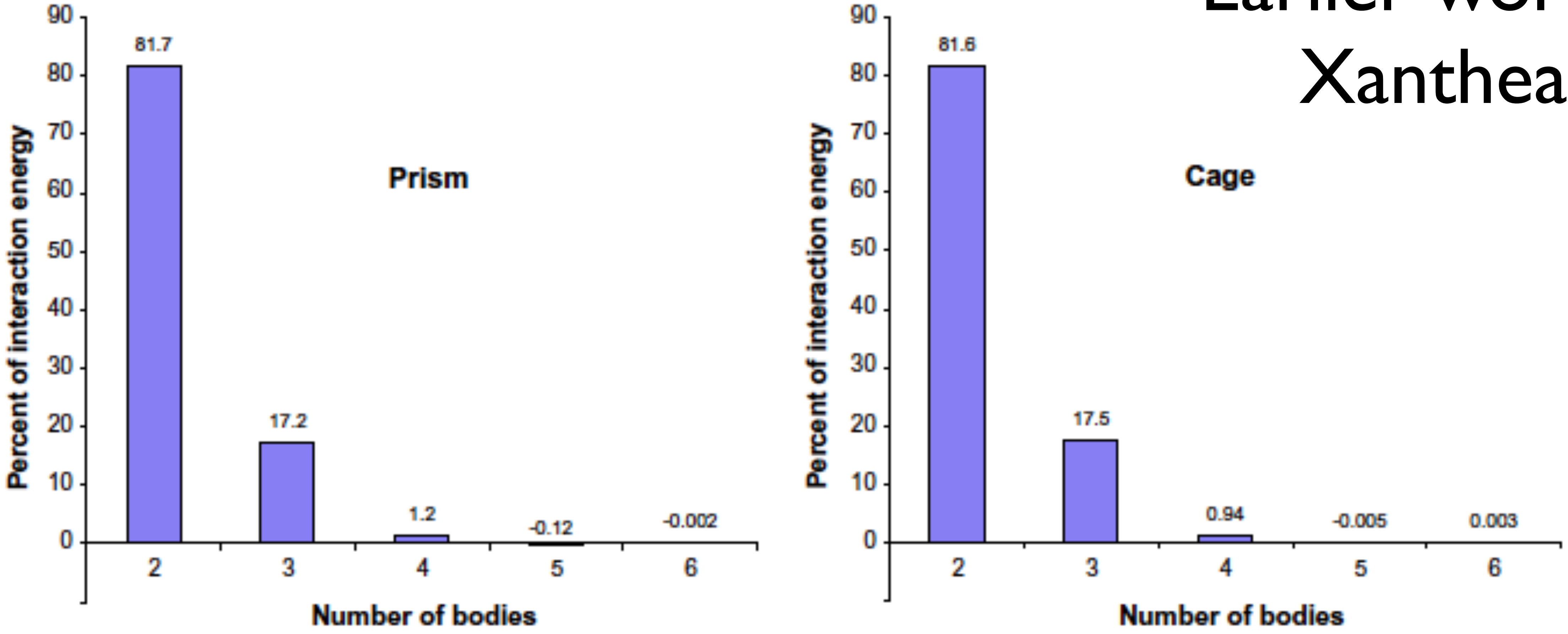

Fig. 1. Convergence of the many-body expansion for the two lowest-energy conformations of the water hexamer [35]. The geometry of each configuration was optimized using the CC-pol-8s plus 3B(SAPT) potential including a polarization model for higher nonadditive terms. At the optimized geometries, calculations were performed with the CCSD(T) method. The pair contributions were computed at the CBS level, all higher-body contributions using an augmented near-triple-zeta quality basis set.

The Water Potential

Flexible, *ab initio* potential and dipole moment surfaces for water. I. Tests and applications for clusters up to the 22-mer, J. Chem. Phys. Y. Wang *et al*. (2011).

$V_{\text{1-body}}(i)$ from Partridge-Schwenke

$V_{\text{2-body}}(i, j)$ from 30 000 CCSD(T)/avtz

$V_{\text{3-body}}(i, j, k)$ from 40 000 MP2/avtz

2 and 3-body fits use permutationally invariant bases

Dipole Moment Surface

$$\vec{\mu}_{\text{dimer}}(\mathrm{X}) = \sum_{i=1}^{6} q_i(\mathrm{X})\vec{r}_i$$

X denotes Cartesians of each atom and dimer dipole = sum of 1-body plus intrinsic 2-body terms.

$$\mathrm{DMS}(1,2) = \sum_{k} \vec{\mu}_{\text{1-body}}(k) + \sum_{k<l} \vec{\mu}_{\text{2-body}}(k,l).$$

J. Phys. Chem. A 2006, 110, 445−451

Ab Initio Potential Energy and Dipole Moment Surfaces of $(H_2O)_2$[†]

Xinchuan Huang,[‡] Bastiaan J. Braams,[‡,§] and Joel M. Bowman*[‡]

$S_2 \times S_4 = 48$ Roughly 30 000 CCSD(T)/aug-cc-pVTZ energies

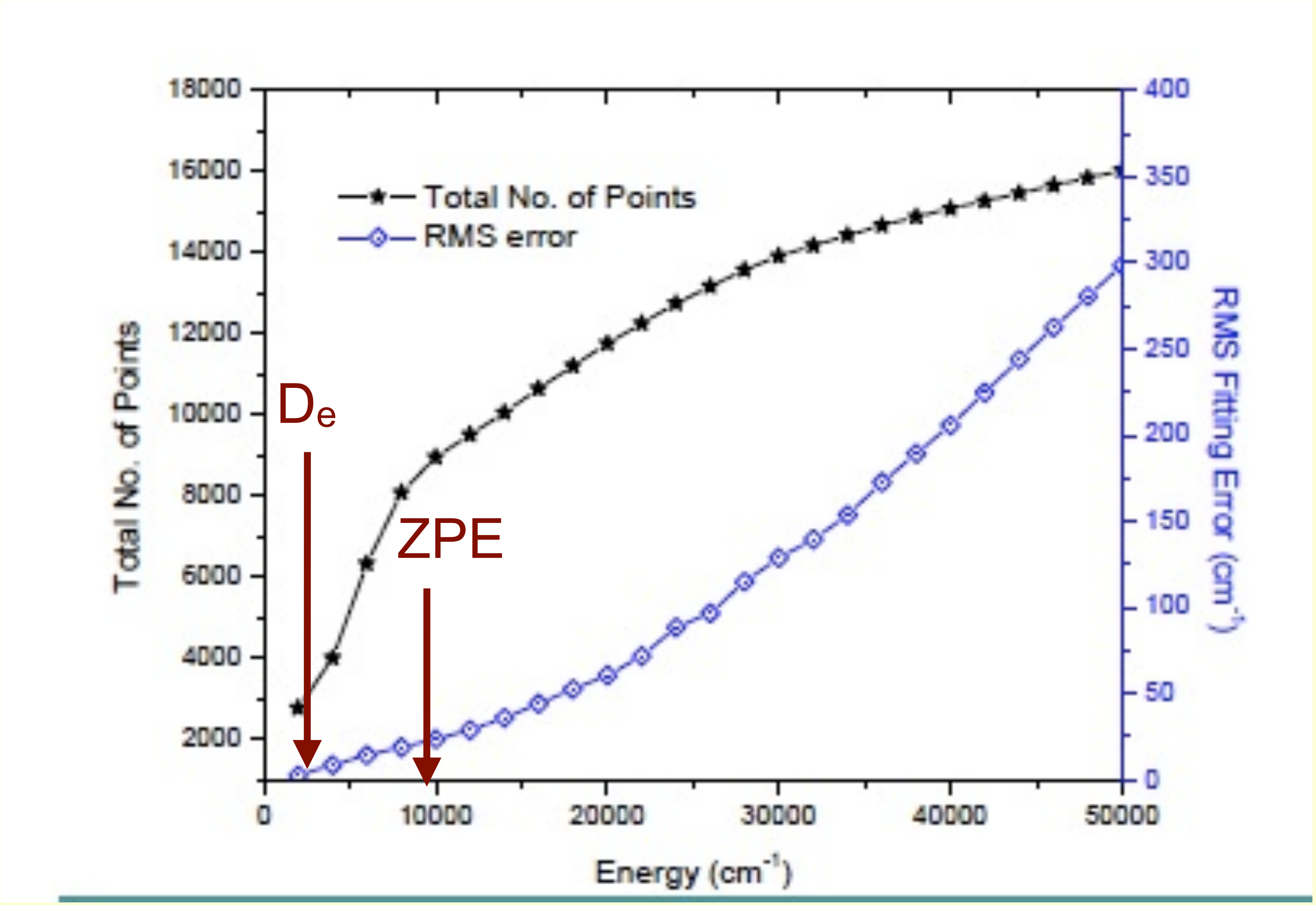

2-body Potentials

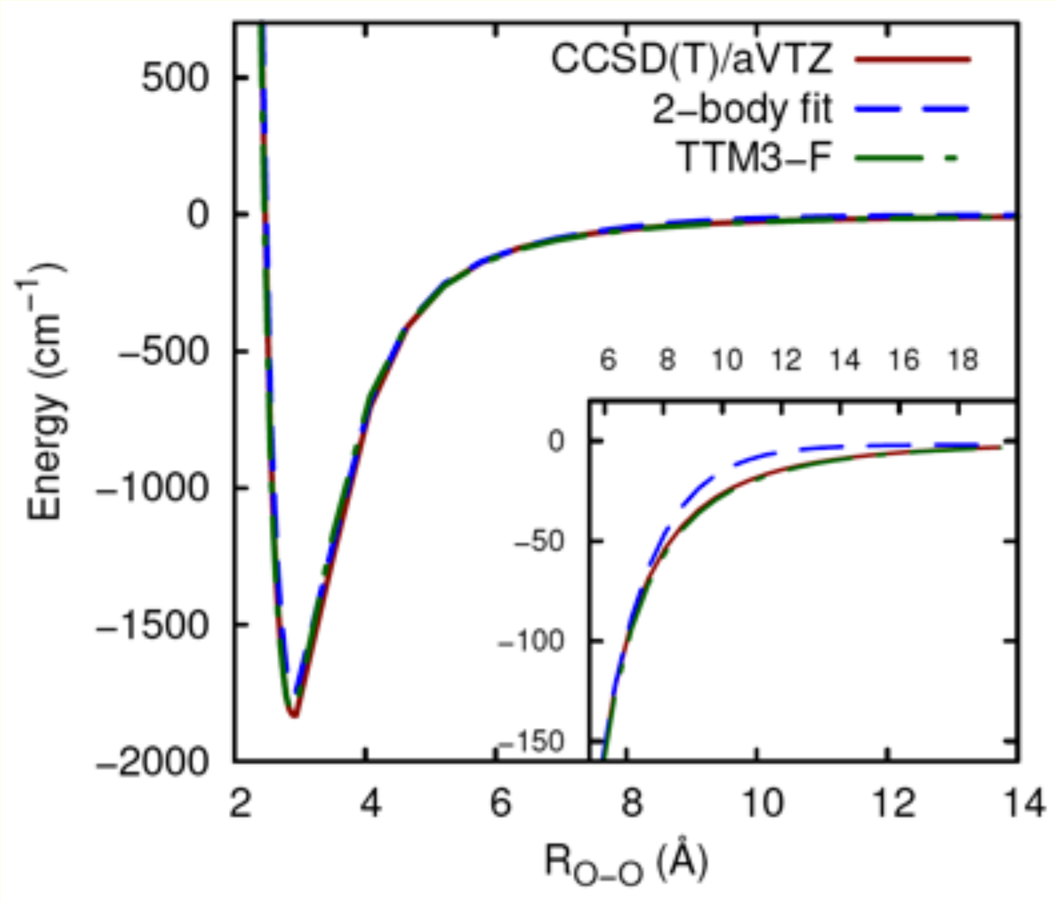

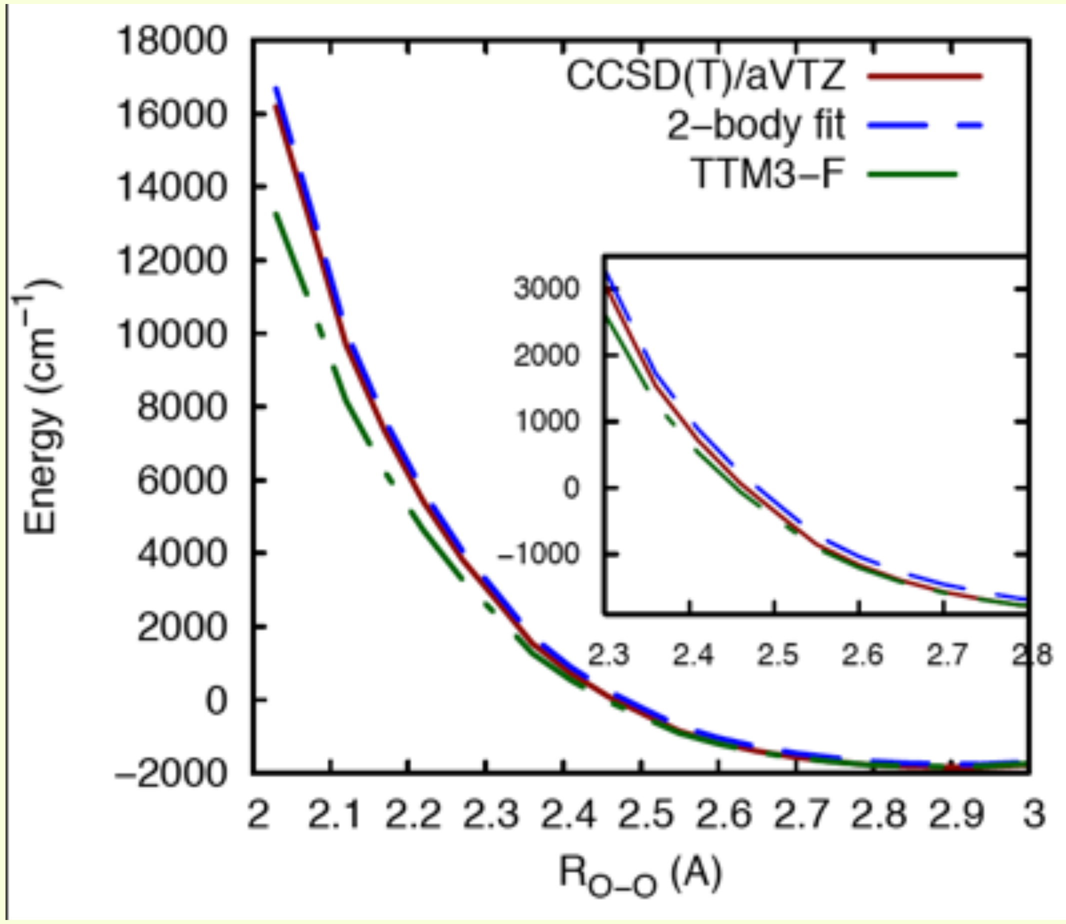

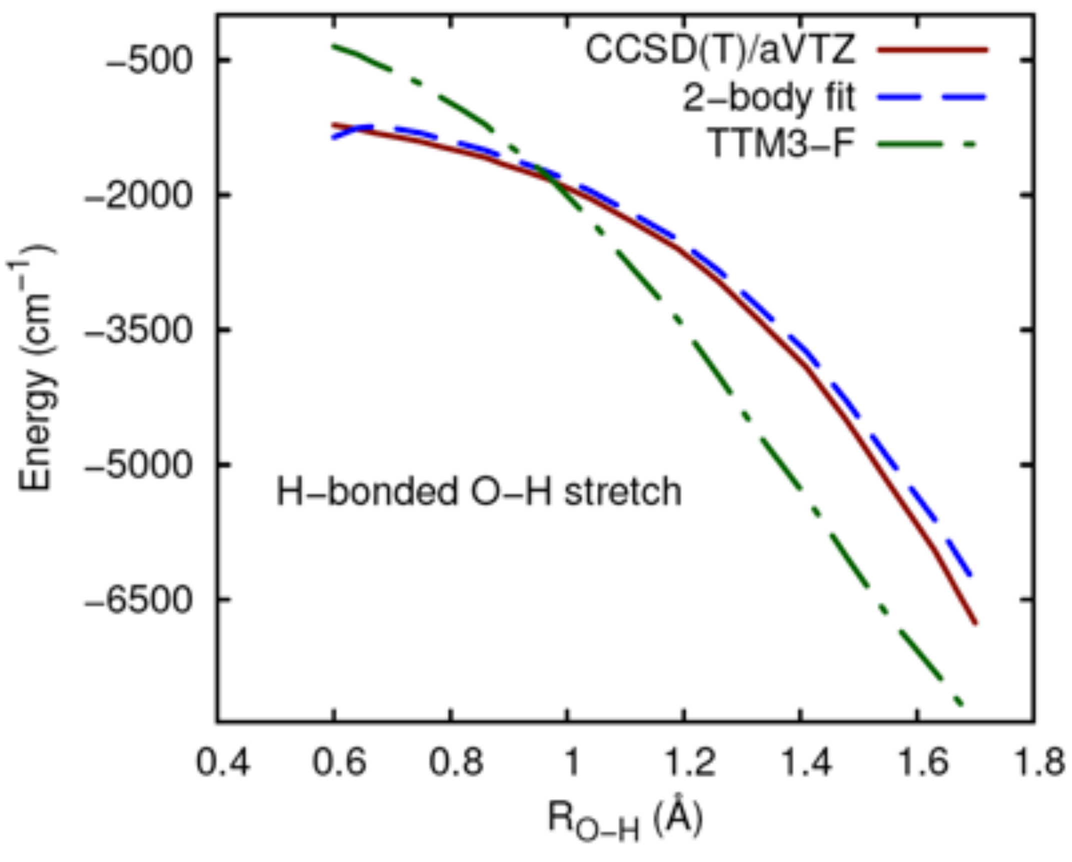

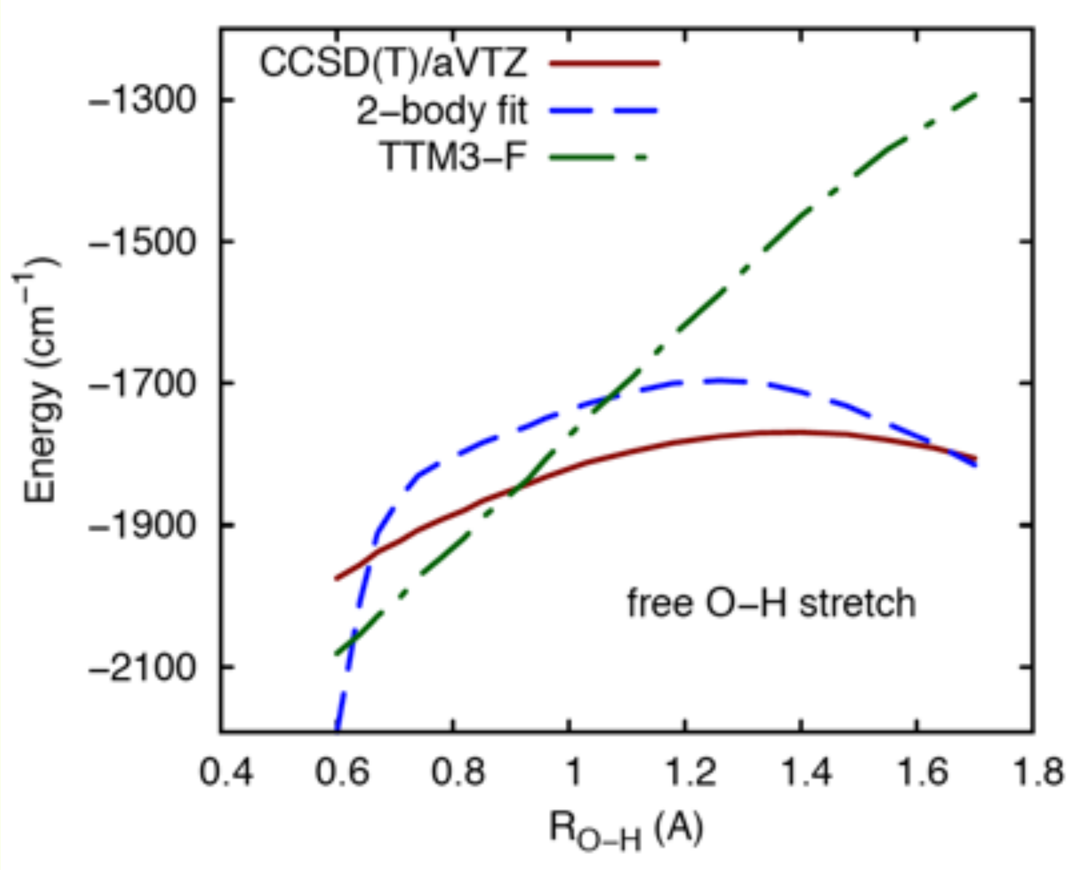

Water Dimer Stationary Points

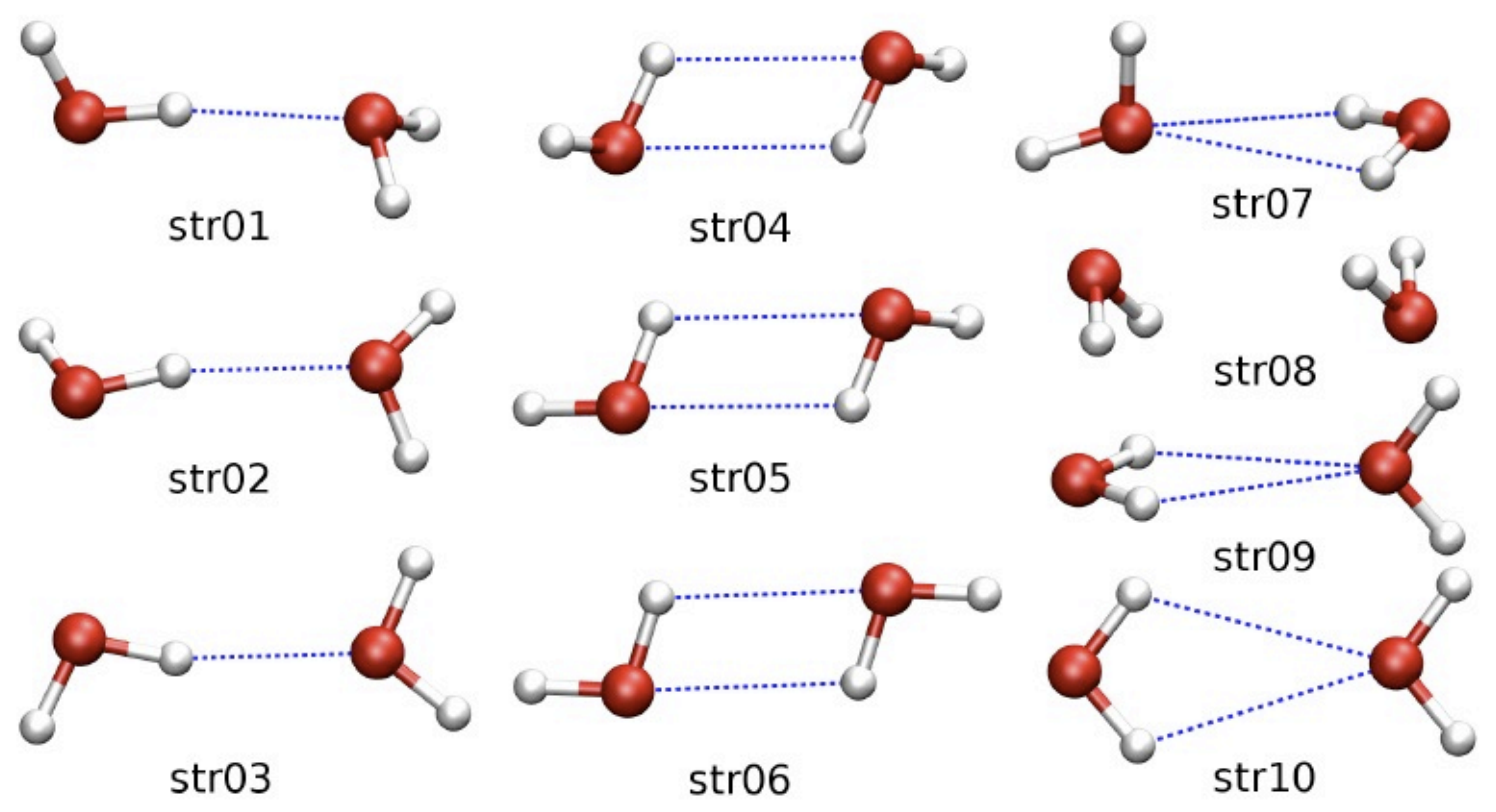

12 vibrational dofs, 15 Morse variables

NN DFT* and PI CCSD(T) water dimer stationary pts (cm^{-1})

NN	DFT	PI	CCSD(T)
232	231	164	163
285	294	197	197
367	371	244	246
490	493	328	328
612	612	346	346
787	790	601	601
1306	1311	1186	1176
747	741	589	589
1079	1077	897	899

* DFT/PBE

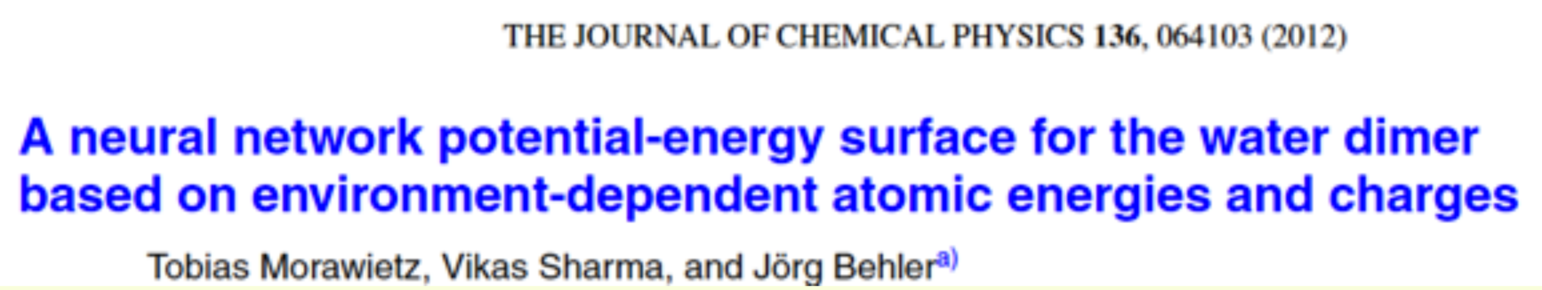

THE JOURNAL OF CHEMICAL PHYSICS 136, 064103 (2012)

A neural network potential-energy surface for the water dimer based on environment-dependent atomic energies and charges

Tobias Morawietz, Vikas Sharma, and Jörg Behler[a)]

Theory and Experiment Agree on D_0 for $(H_2O)_2$

THE JOURNAL OF CHEMICAL PHYSICS 130, 144314 (2009)

Accurate *ab initio* and "hybrid" potential energy surfaces, intramolecular vibrational energies, and classical ir spectrum of the water dimer

Alex Shank, Yimin Wang, Alexey Kaledin, Bastiaan J. Braams, and Joel M. Bowman[a)]
Department of Chemistry and Cherry L. Emerson Center for Scientific Computation,
Emory University, Atlanta, Georgia 30322, USA

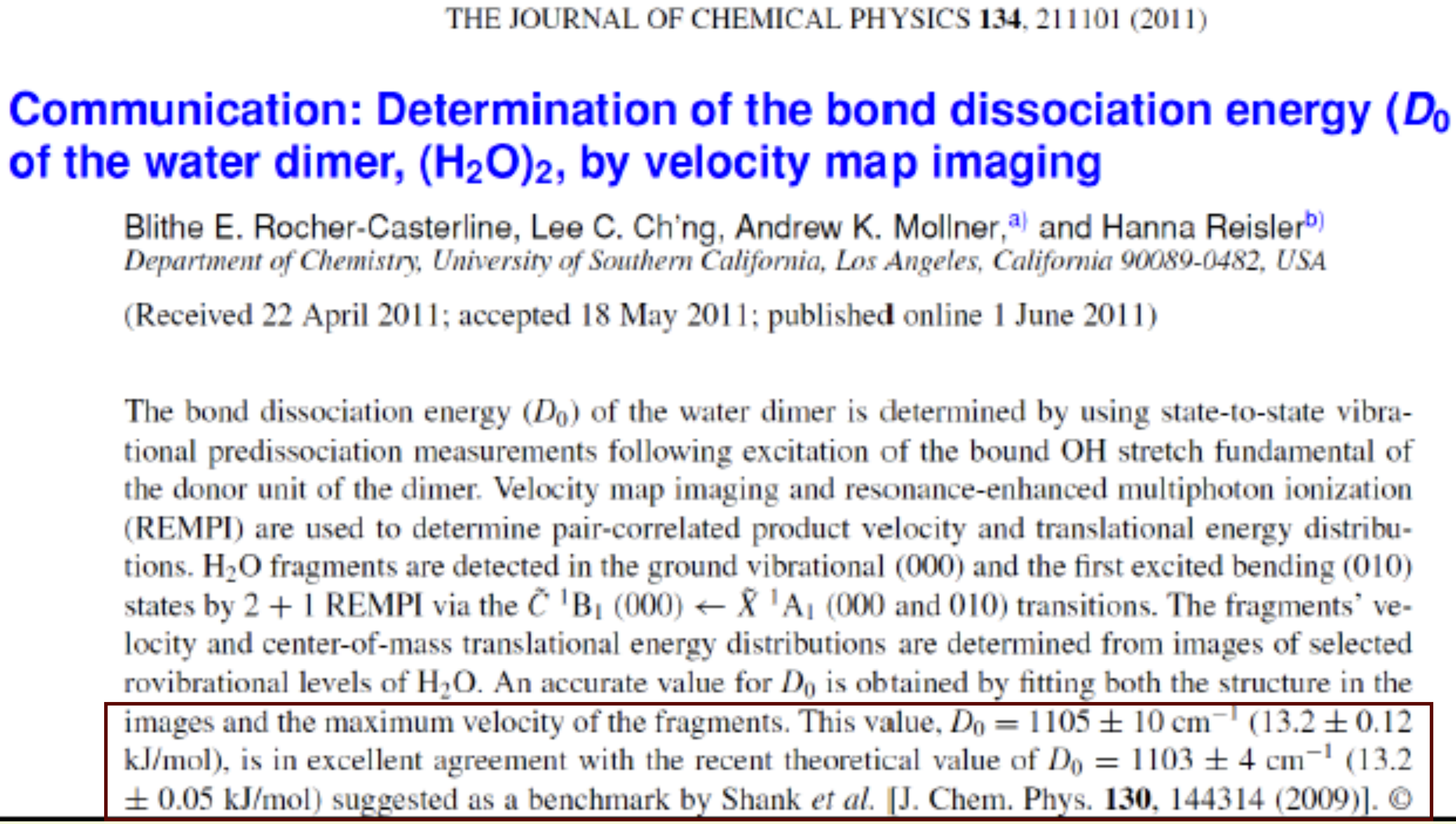

THE JOURNAL OF CHEMICAL PHYSICS **134**, 211101 (2011)

Communication: Determination of the bond dissociation energy (D_0 of the water dimer, $(H_2O)_2$, by velocity map imaging

Blithe E. Rocher-Casterline, Lee C. Ch'ng, Andrew K. Mollner,[a)] and Hanna Reisler[b)]
Department of Chemistry, University of Southern California, Los Angeles, California 90089-0482, USA

(Received 22 April 2011; accepted 18 May 2011; published online 1 June 2011)

The bond dissociation energy (D_0) of the water dimer is determined by using state-to-state vibrational predissociation measurements following excitation of the bound OH stretch fundamental of the donor unit of the dimer. Velocity map imaging and resonance-enhanced multiphoton ionization (REMPI) are used to determine pair-correlated product velocity and translational energy distributions. H_2O fragments are detected in the ground vibrational (000) and the first excited bending (010) states by 2 + 1 REMPI via the $\tilde{C}\ ^1B_1$ (000) ← $\tilde{X}\ ^1A_1$ (000 and 010) transitions. The fragments' velocity and center-of-mass translational energy distributions are determined from images of selected rovibrational levels of H_2O. An accurate value for D_0 is obtained by fitting both the structure in the images and the maximum velocity of the fragments. This value, $D_0 = 1105 \pm 10\ \mathrm{cm}^{-1}$ (13.2 ± 0.12 kJ/mol), is in excellent agreement with the recent theoretical value of $D_0 = 1103 \pm 4\ \mathrm{cm}^{-1}$ (13.2 ± 0.05 kJ/mol) suggested as a benchmark by Shank *et al.* [J. Chem. Phys. **130**, 144314 (2009)]. ©

3b from the Water Trimer

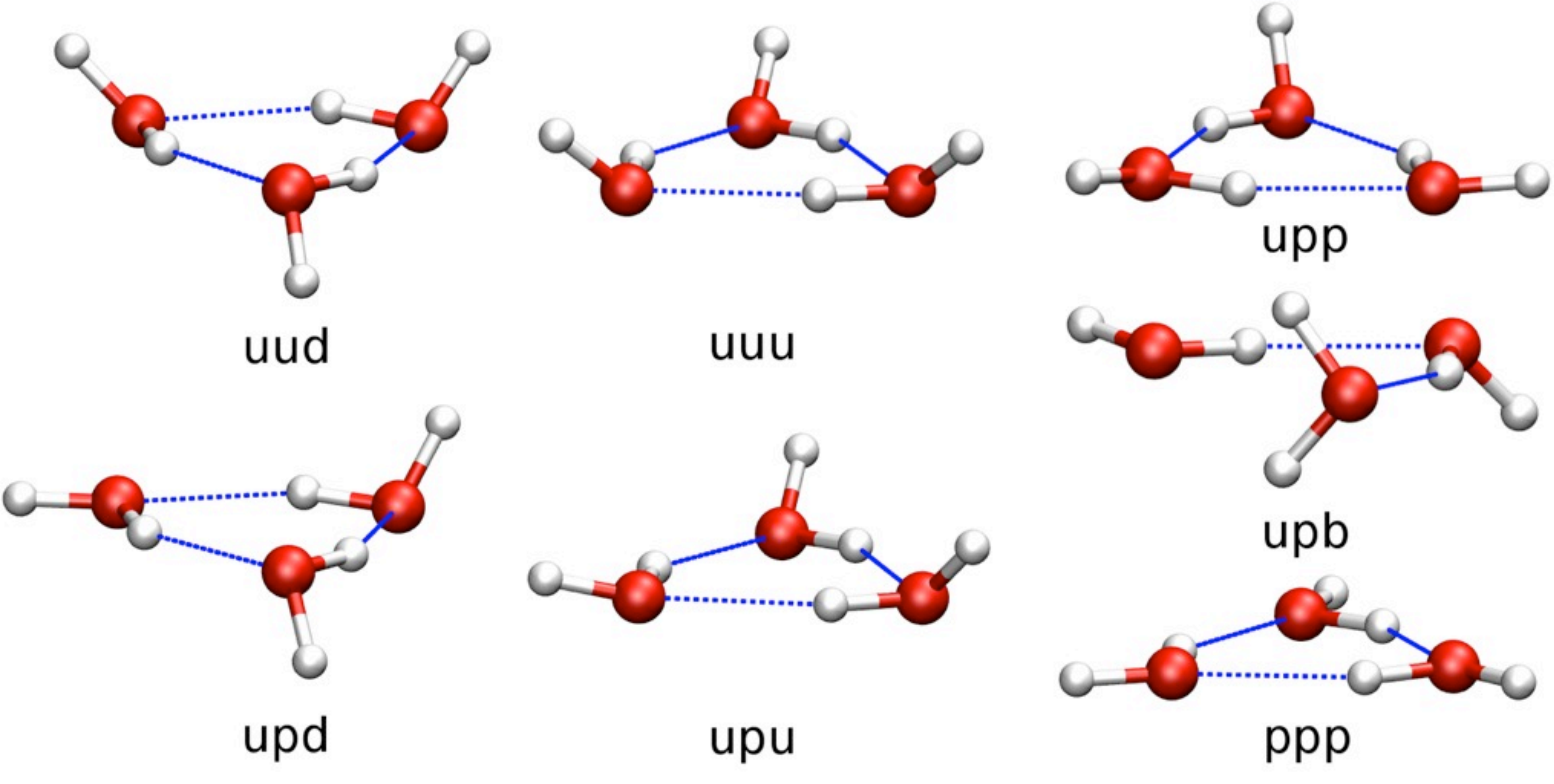

21 vibrational dofs, 36 Morse variables.
5th and 6th order fits

3-body potential (36 variables)

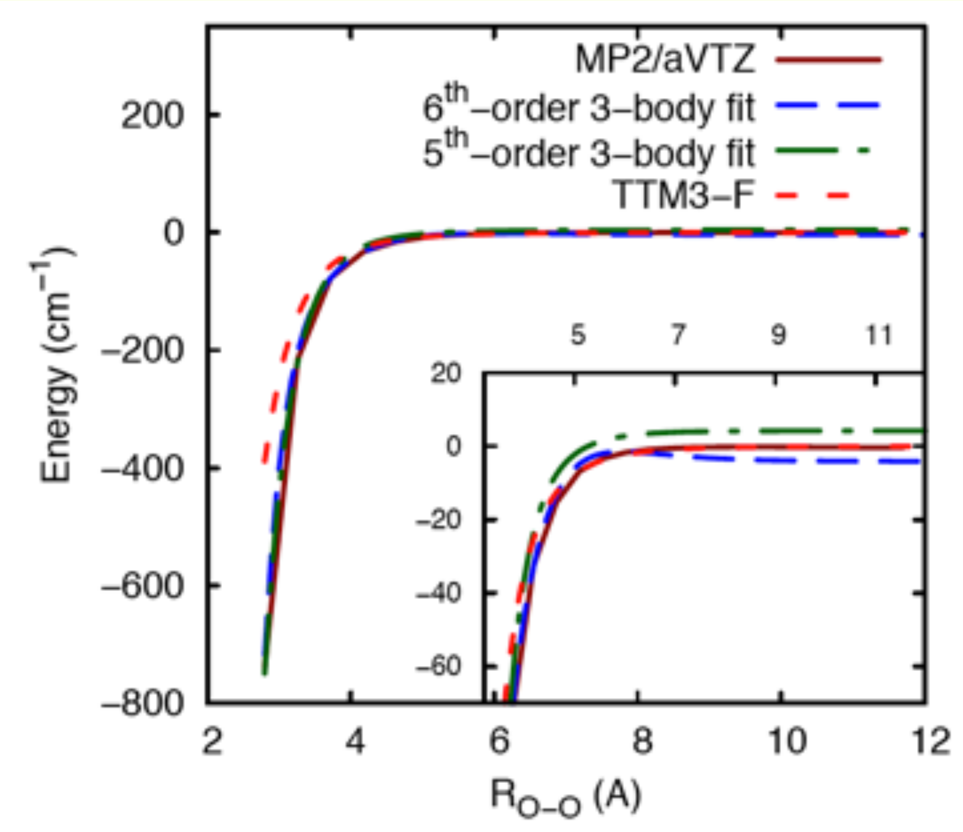

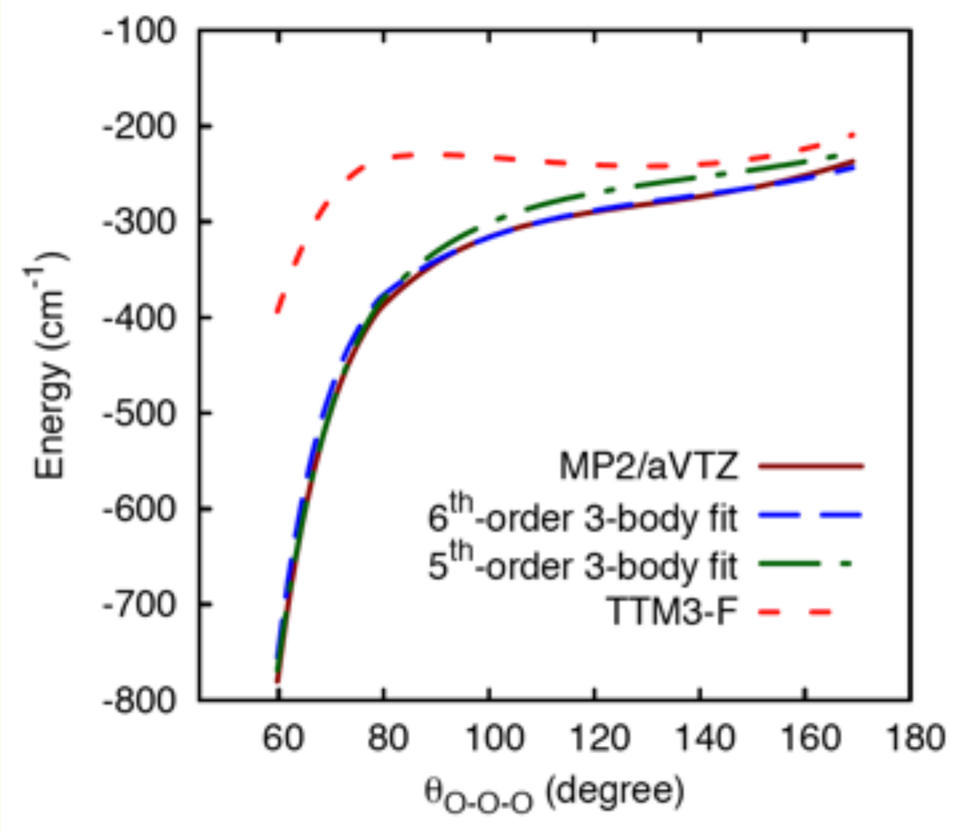

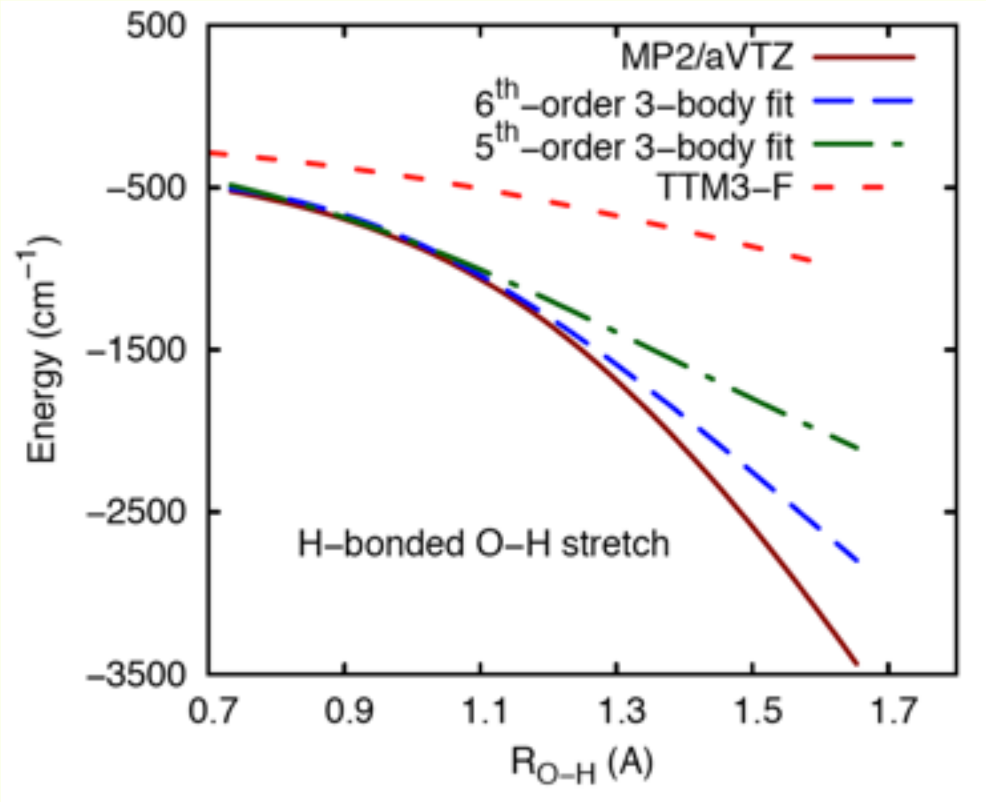

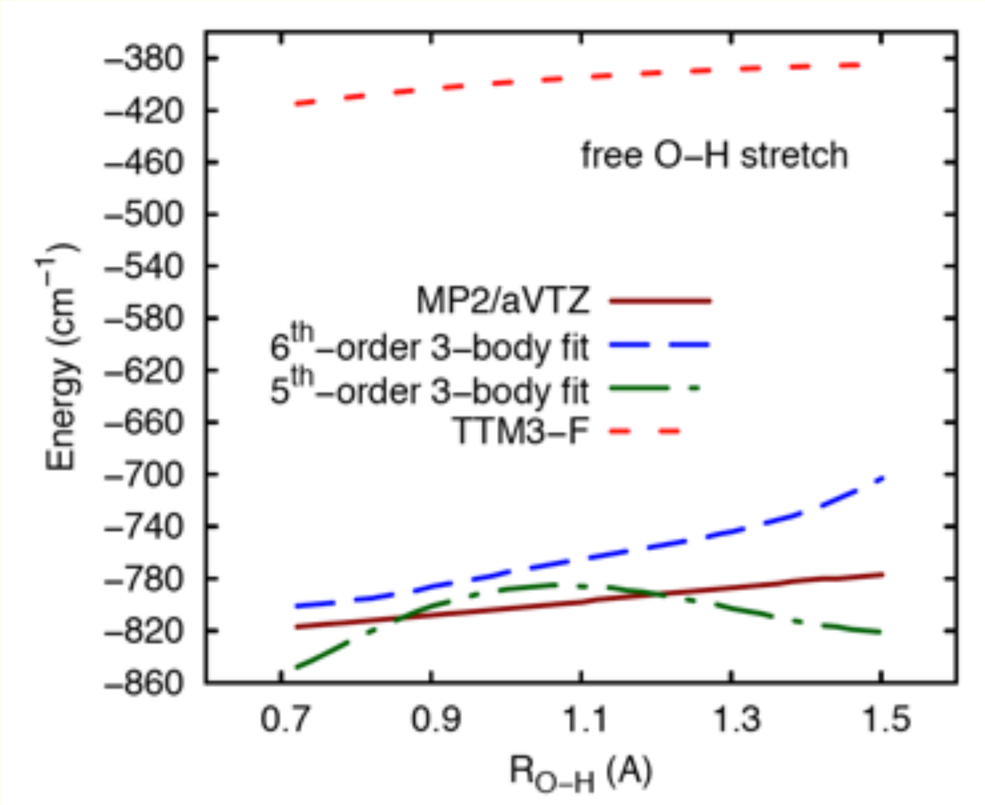

Fitting the dipole moment

Consider H_2O as an example

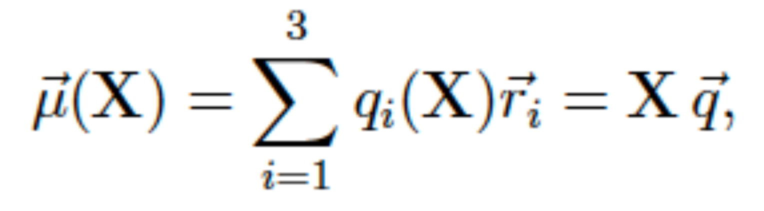

$$\vec{\mu}(\mathbf{X}) = \sum_{i=1}^{3} q_i(\mathbf{X})\vec{r}_i = \mathbf{X}\,\vec{q},$$

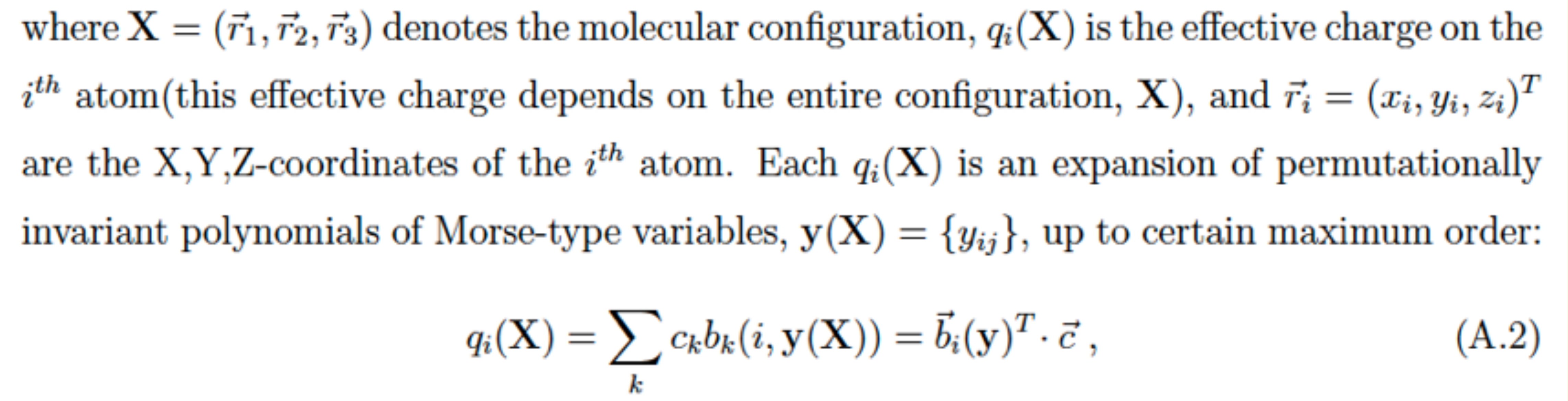

where $\mathbf{X} = (\vec{r}_1, \vec{r}_2, \vec{r}_3)$ denotes the molecular configuration, $q_i(\mathbf{X})$ is the effective charge on the i^{th} atom(this effective charge depends on the entire configuration, $\mathbf{X}$), and $\vec{r}_i = (x_i, y_i, z_i)^T$ are the X,Y,Z-coordinates of the i^{th} atom. Each $q_i(\mathbf{X})$ is an expansion of permutationally invariant polynomials of Morse-type variables, $\mathbf{y}(\mathbf{X}) = \{y_{ij}\}$, up to certain maximum order:

$$q_i(\mathbf{X}) = \sum_k c_k b_k(i, \mathbf{y}(\mathbf{X})) = \vec{b}_i(\mathbf{y})^T \cdot \vec{c}\ , \tag{A.2}$$

Permute the two H atoms

a) and the charge on oxygen doesn't change, so it is invariant just as the PES is to this permutation. So q_3 must be invariant as illustrated by (A.6).

b) q_1 and q_2 must interchange , so not invariant but co-variant. So representation is "general" i.e., but coefficients are equal. This is seen in (A.4) and (A.5). Then finally the dipole is represented by A.7 ready for fitting.

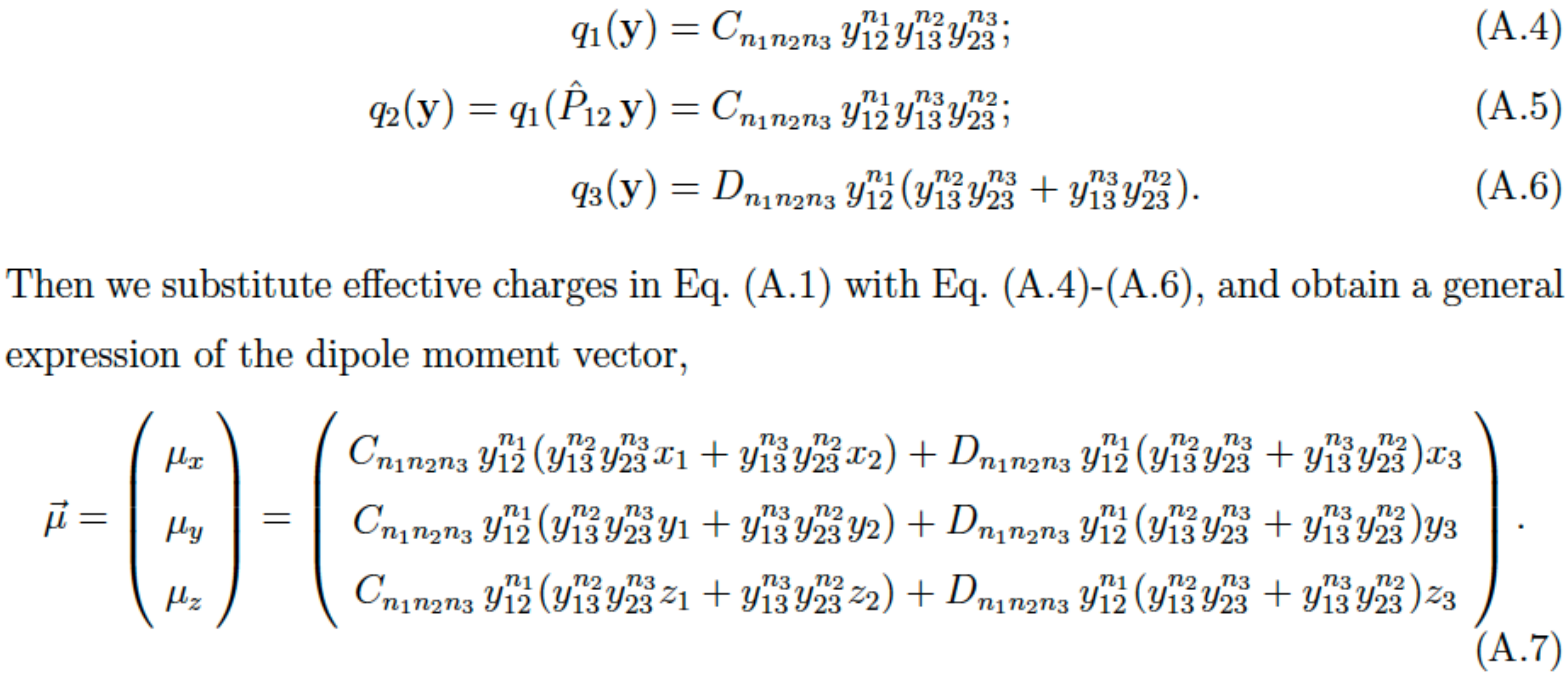

$$q_1(\mathbf{y}) = C_{n_1 n_2 n_3}\, y_{12}^{n_1} y_{13}^{n_2} y_{23}^{n_3}; \tag{A.4}$$

$$q_2(\mathbf{y}) = q_1(\hat{P}_{12}\,\mathbf{y}) = C_{n_1 n_2 n_3}\, y_{12}^{n_1} y_{13}^{n_3} y_{23}^{n_2}; \tag{A.5}$$

$$q_3(\mathbf{y}) = D_{n_1 n_2 n_3}\, y_{12}^{n_1} (y_{13}^{n_2} y_{23}^{n_3} + y_{13}^{n_3} y_{23}^{n_2}). \tag{A.6}$$

Then we substitute effective charges in Eq. (A.1) with Eq. (A.4)-(A.6), and obtain a general expression of the dipole moment vector,

$$\vec{\mu} = \begin{pmatrix} \mu_x \\ \mu_y \\ \mu_z \end{pmatrix} = \begin{pmatrix} C_{n_1 n_2 n_3}\, y_{12}^{n_1} (y_{13}^{n_2} y_{23}^{n_3} x_1 + y_{13}^{n_3} y_{23}^{n_2} x_2) + D_{n_1 n_2 n_3}\, y_{12}^{n_1} (y_{13}^{n_2} y_{23}^{n_3} + y_{13}^{n_3} y_{23}^{n_2}) x_3 \\ C_{n_1 n_2 n_3}\, y_{12}^{n_1} (y_{13}^{n_2} y_{23}^{n_3} y_1 + y_{13}^{n_3} y_{23}^{n_2} y_2) + D_{n_1 n_2 n_3}\, y_{12}^{n_1} (y_{13}^{n_2} y_{23}^{n_3} + y_{13}^{n_3} y_{23}^{n_2}) y_3 \\ C_{n_1 n_2 n_3}\, y_{12}^{n_1} (y_{13}^{n_2} y_{23}^{n_3} z_1 + y_{13}^{n_3} y_{23}^{n_2} z_2) + D_{n_1 n_2 n_3}\, y_{12}^{n_1} (y_{13}^{n_2} y_{23}^{n_3} + y_{13}^{n_3} y_{23}^{n_2}) z_3 \end{pmatrix}. \tag{A.7}$$

Dipole Moment Tests

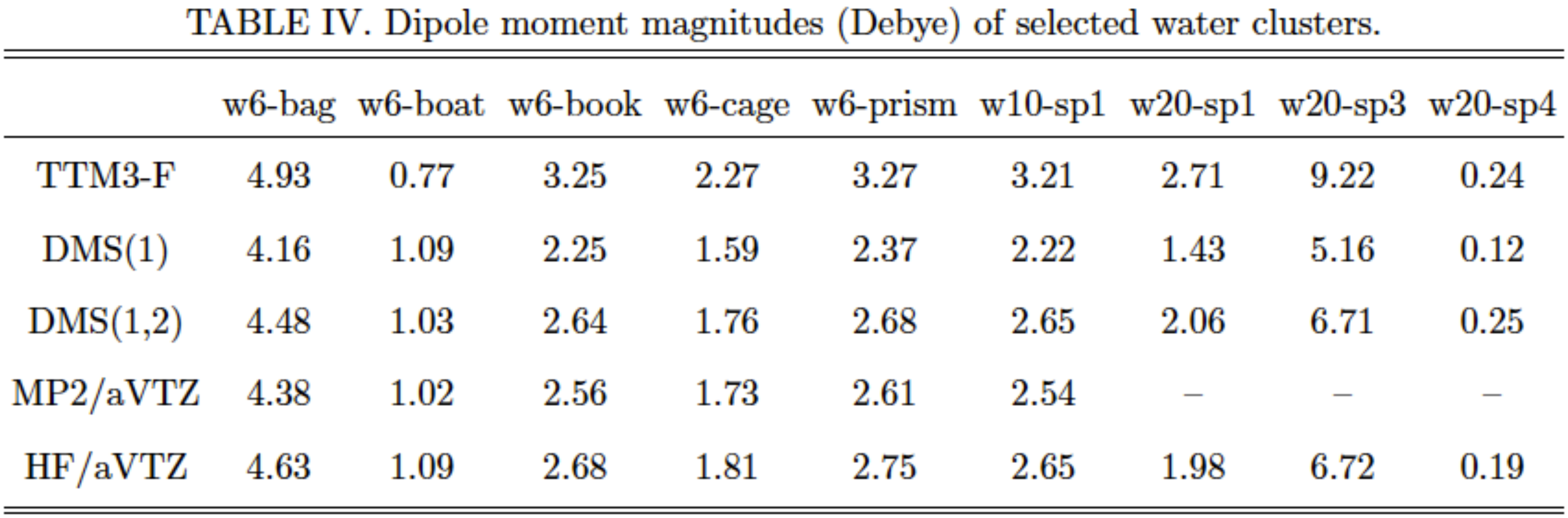

TABLE IV. Dipole moment magnitudes (Debye) of selected water clusters.

	w6-bag	w6-boat	w6-book	w6-cage	w6-prism	w10-sp1	w20-sp1	w20-sp3	w20-sp4
TTM3-F	4.93	0.77	3.25	2.27	3.27	3.21	2.71	9.22	0.24
DMS(1)	4.16	1.09	2.25	1.59	2.37	2.22	1.43	5.16	0.12
DMS(1,2)	4.48	1.03	2.64	1.76	2.68	2.65	2.06	6.71	0.25
MP2/aVTZ	4.38	1.02	2.56	1.73	2.61	2.54	–	–	–
HF/aVTZ	4.63	1.09	2.68	1.81	2.75	2.65	1.98	6.72	0.19

Comments

1. TTM3-F uses a standard polarization model for the induced dipole
2. We are developing a variable point charge model that reproduces the above dipoles as well or better than TTM3-F

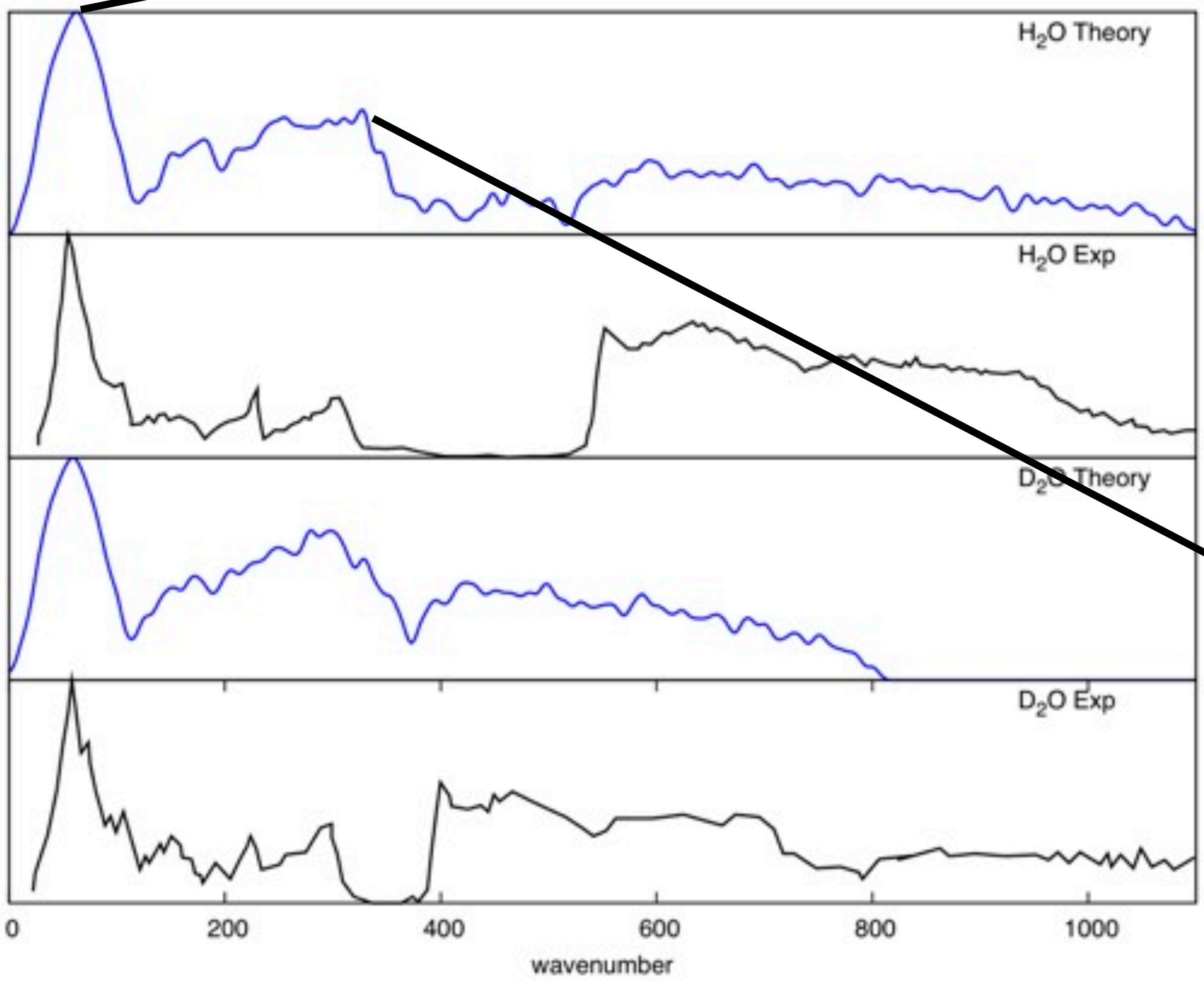

~50 cm-1
"In-phase", or "acoustic"

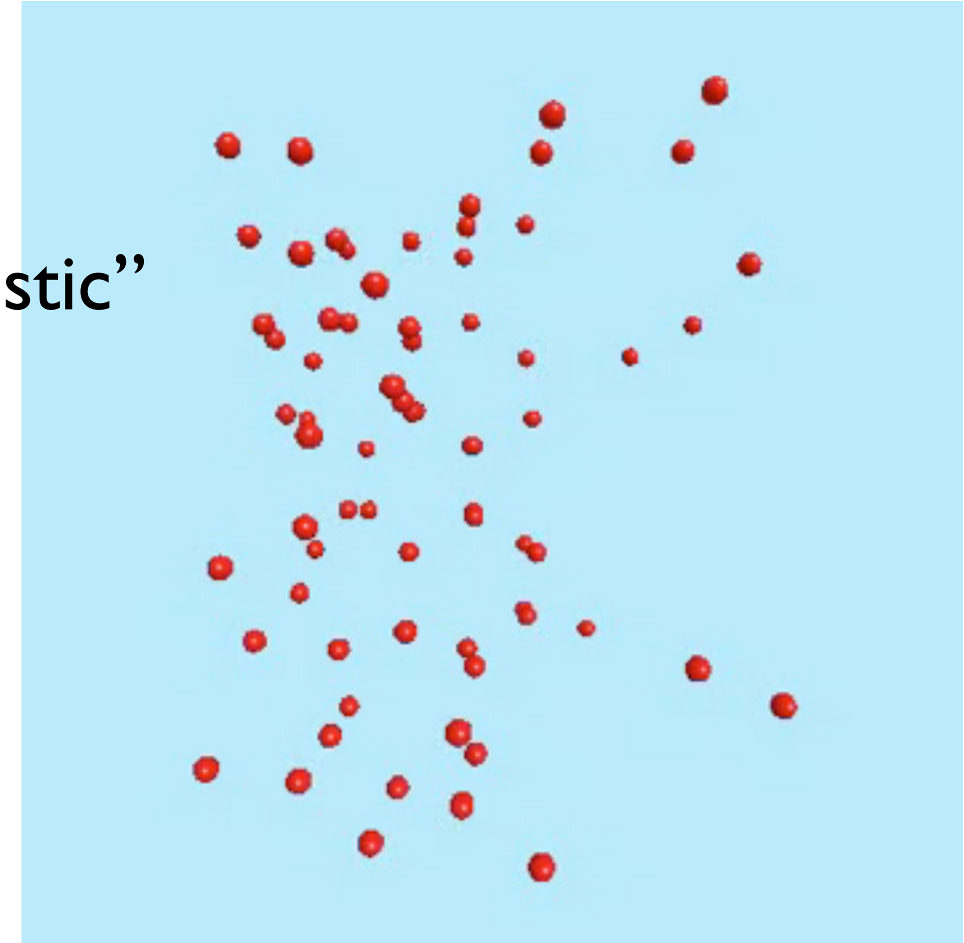

~300 cm-1
"Out-of-phase", or "optic"

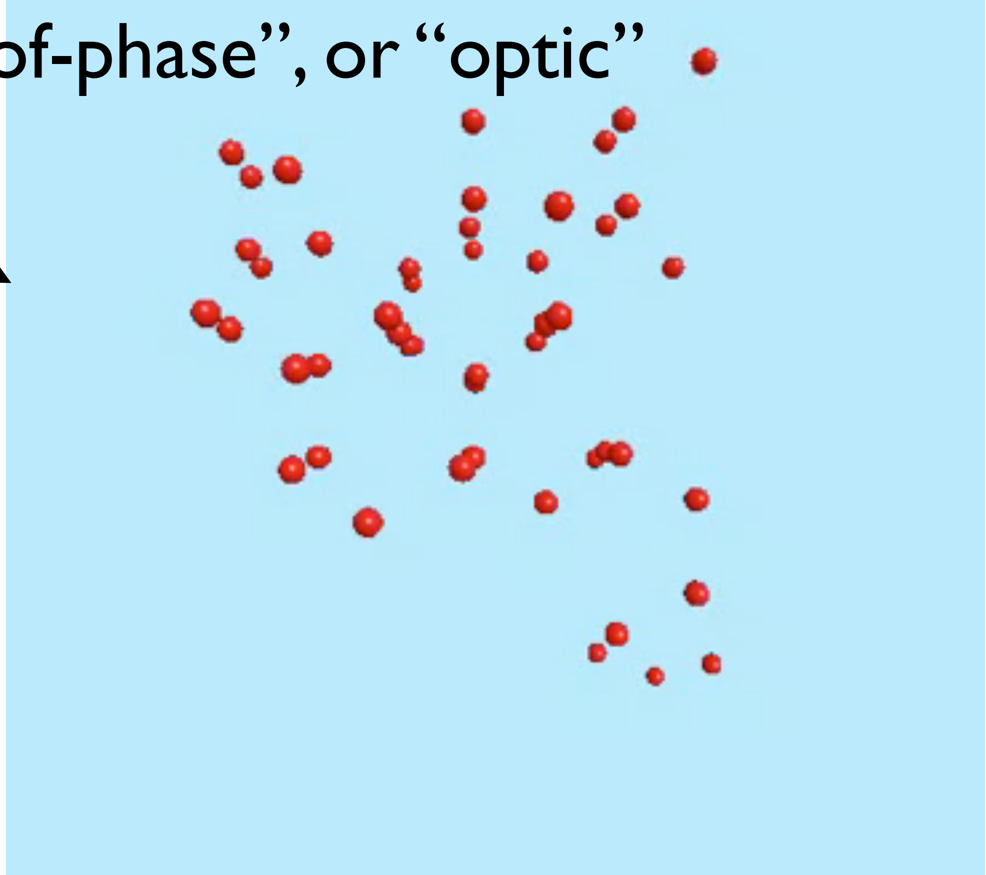

Force Fields

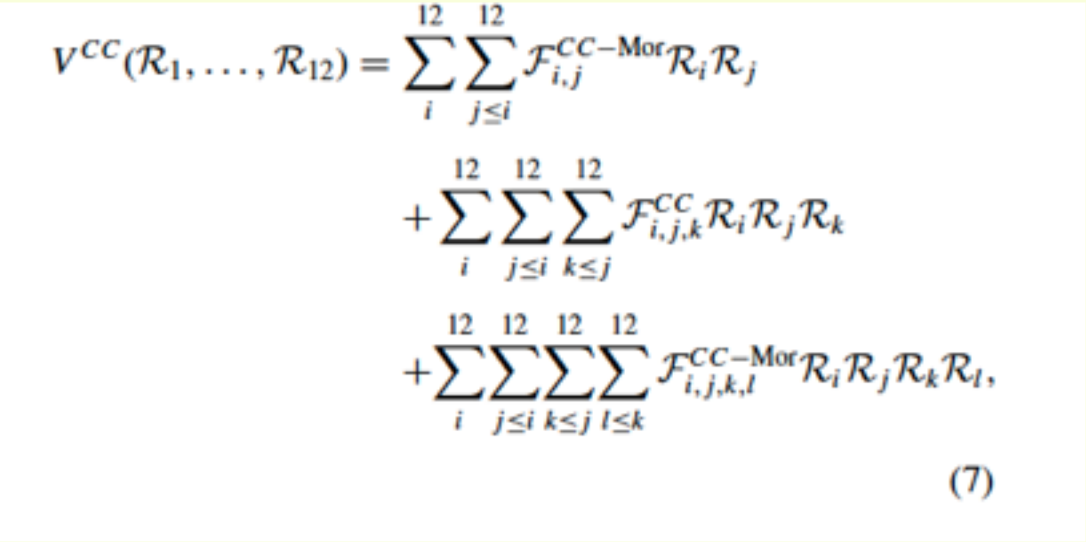

$$V^{CC}(\mathcal{R}_1,\ldots,\mathcal{R}_{12}) = \sum_{i}^{12}\sum_{j\le i}^{12}\mathcal{F}_{i,j}^{CC-\mathrm{Mor}}\mathcal{R}_i\mathcal{R}_j + \sum_{i}^{12}\sum_{j\le i}^{12}\sum_{k\le j}^{12}\mathcal{F}_{i,j,k}^{CC}\mathcal{R}_i\mathcal{R}_j\mathcal{R}_k + \sum_{i}^{12}\sum_{j\le i}^{12}\sum_{k\le j}^{12}\sum_{l\le k}^{12}\mathcal{F}_{i,j,k,l}^{CC-\mathrm{Mor}}\mathcal{R}_i\mathcal{R}_j\mathcal{R}_k\mathcal{R}_l, \tag{7}$$

C_2H_4 Martin and Lee VPT2

Looks like a Taylor series about the equilibrium.

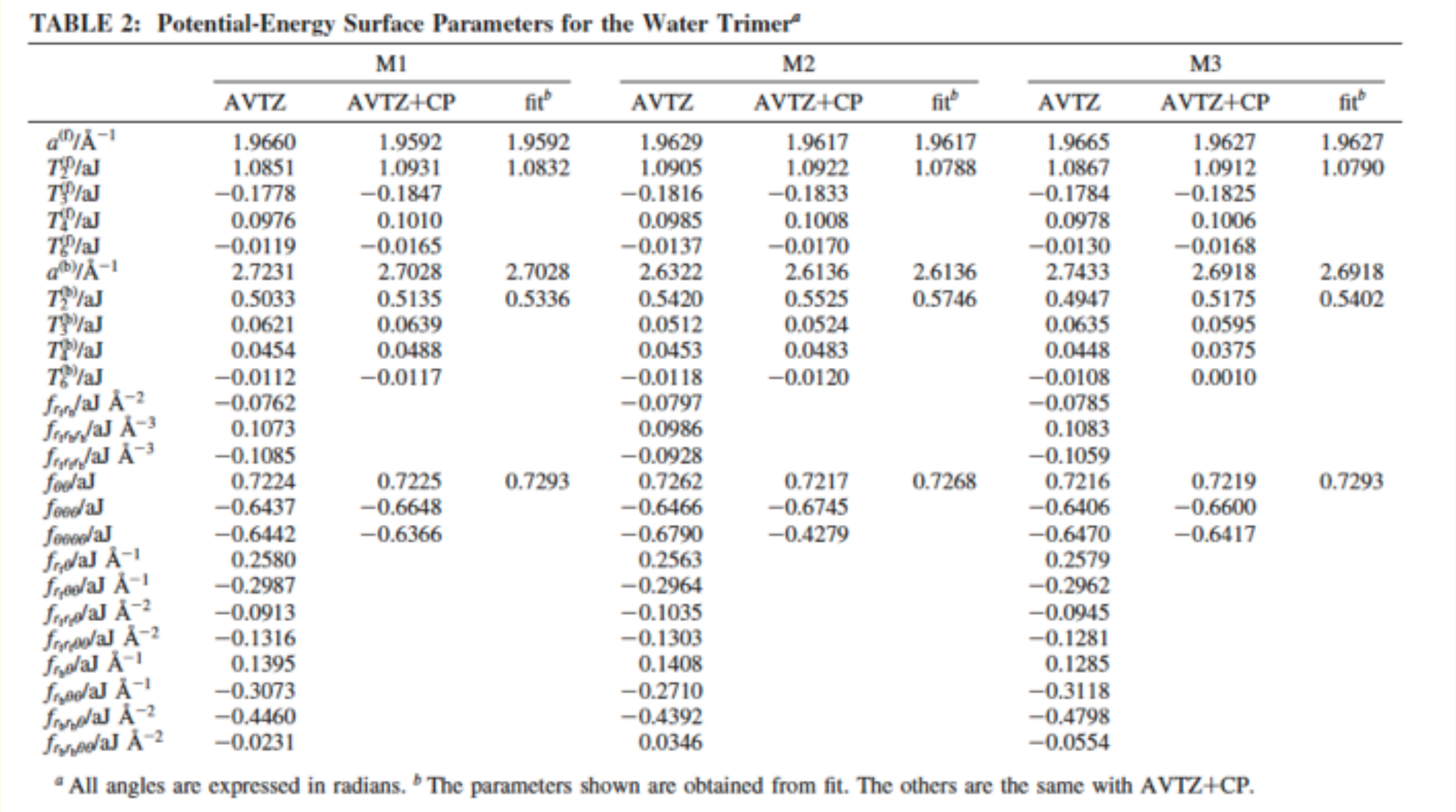

TABLE 2: Potential-Energy Surface Parameters for the Water Trimer[a]

	M1			M2			M3		
	AVTZ	AVTZ+CP	fit[b]	AVTZ	AVTZ+CP	fit[b]	AVTZ	AVTZ+CP	fit[b]
$a^{(f)}$/Å^{-1}	1.9660	1.9592	1.9592	1.9629	1.9617	1.9617	1.9665	1.9627	1.9627
$T_2^{(f)}$/aJ	1.0851	1.0931	1.0832	1.0905	1.0922	1.0788	1.0867	1.0912	1.0790
$T_3^{(f)}$/aJ	−0.1778	−0.1847		−0.1816	−0.1833		−0.1784	−0.1825	
$T_4^{(f)}$/aJ	0.0976	0.1010		0.0985	0.1008		0.0978	0.1006	
$T_6^{(f)}$/aJ	−0.0119	−0.0165		−0.0137	−0.0170		−0.0130	−0.0168	
$a^{(b)}$/Å^{-1}	2.7231	2.7028	2.7028	2.6322	2.6136	2.6136	2.7433	2.6918	2.6918
$T_2^{(b)}$/aJ	0.5033	0.5135	0.5336	0.5420	0.5525	0.5746	0.4947	0.5175	0.5402
$T_3^{(b)}$/aJ	0.0621	0.0639		0.0512	0.0524		0.0635	0.0595	
$T_4^{(b)}$/aJ	0.0454	0.0488		0.0453	0.0483		0.0448	0.0375	
$T_6^{(b)}$/aJ	−0.0112	−0.0117		−0.0118	−0.0120		−0.0108	0.0010	
$f_{r_f r_b}$/aJ Å^{-2}	−0.0762			−0.0797			−0.0785		
$f_{r_f r_b r_b}$/aJ Å^{-3}	0.1073			0.0986			0.1083		
$f_{r_f r_f r_b}$/aJ Å^{-3}	−0.1085			−0.0928			−0.1059		
$f_{\theta\theta}$/aJ	0.7224	0.7225	0.7293	0.7262	0.7217	0.7268	0.7216	0.7219	0.7293
$f_{\theta\theta\theta}$/aJ	−0.6437	−0.6648		−0.6466	−0.6745		−0.6406	−0.6600	
$f_{\theta\theta\theta\theta}$/aJ	−0.6442	−0.6366		−0.6790	−0.4279		−0.6470	−0.6417	
$f_{r_f\theta}$/aJ Å^{-1}	0.2580			0.2563			0.2579		
$f_{r_f\theta\theta}$/aJ Å^{-1}	−0.2987			−0.2964			−0.2962		
$f_{r_f r_f\theta}$/aJ Å^{-2}	−0.0913			−0.1035			−0.0945		
$f_{r_f r_f\theta\theta}$/aJ Å^{-2}	−0.1316			−0.1303			−0.1281		
$f_{r_b\theta}$/aJ Å^{-1}	0.1395			0.1408			0.1285		
$f_{r_b\theta\theta}$/aJ Å^{-1}	−0.3073			−0.2710			−0.3118		
$f_{r_b r_b\theta}$/aJ Å^{-2}	−0.4460			−0.4392			−0.4798		
$f_{r_b r_b\theta\theta}$/aJ Å^{-2}	−0.0231			0.0346			−0.0554		

[a] All angles are expressed in radians. [b] The parameters shown are obtained from fit. The others are the same with AVTZ+CP.

Halonen and co-workers

n-mode grids

$$V(Q_1,\cdots Q_N) = \sum_{i} V_i^{(1)}(Q_i) + \sum_{i\neq j} V_{i,j}^{(2)}(Q_i,Q_j) + \sum_{i\neq j\neq k} V_{i,j,k}^{(3)}(Q_i,Q_j,Q_k) + \cdots + \sum_{i\neq j\neq k,\ldots} V_{i,j,k,\ldots}^{(n)}(Q_i,Q_j,Q_k,\ldots)$$

The potential on these grids can be obtained directly by ab initio methods and this is done by a number of groups, even using different levels of ab initio theory.

Then various interpolations can be used in these “low” dimensional functions to get V at say quadrature points.

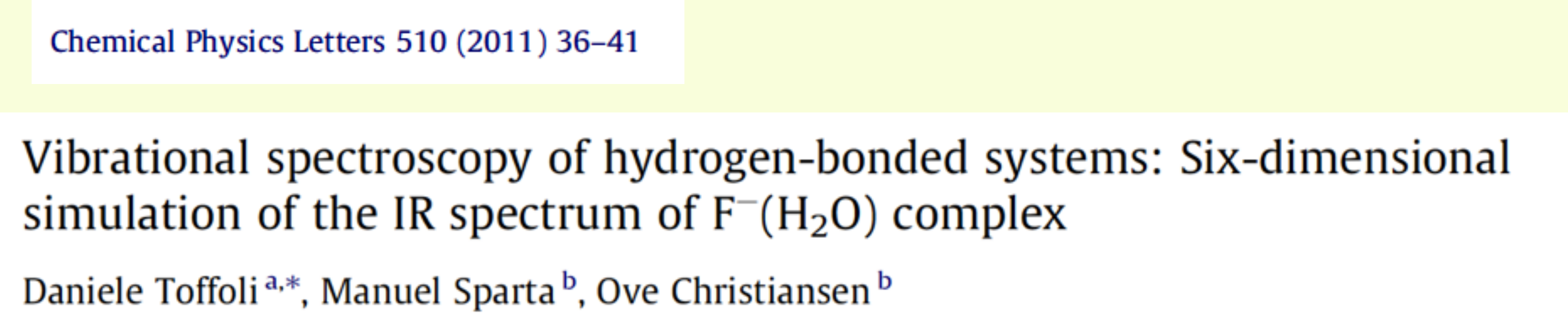

Chemical Physics Letters 510 (2011) 36–41

Vibrational spectroscopy of hydrogen-bonded systems: Six-dimensional simulation of the IR spectrum of $F^-(H_2O)$ complex

Daniele Toffoli [a,*], Manuel Sparta [b], Ove Christiansen [b]